引用格式：唐玄, 云露, 何希鹏, 等. 中国东部咸化湖盆始新统混积页岩岩相及有机质富集机制[J]. 油气藏评价与开发, 2026, 16(6): 1151-1170.
Tang Xuan, Yun Lu, He Xipeng, et al. Lithofacies and organic matter enrichment mechanisms of Eocene mixed shales in saline lacustrine basins, eastern China[J]. Petroleum Reservoir Evaluation and Development, 2026, 16(6): 1151-1170.
DOI: 10.13809/j.cnki.cn32-1825/te.20250105

中国东部咸化湖盆始新统混积页岩岩相及有机质富集机制

唐 玄[1,2], 云 露[3,4], 何希鹏[4,5], 高玉巧[4,6], 刘 飏[7], 关子珩[1,2], 周富彤[1,2], 陈怡冉[1,2], 余光展[1,2], 左 鹏[1,2]
(1.中国地质大学(北京)能源学院,北京 100083;2.自然资源部页岩气资源战略评价重点实验室,北京 100083;
3.中国石化石油勘探开发研究院,北京 102206;4.页岩油气富集机理与高效开发全国重点实验室,北京 102206;
5.中国石化华东油气分公司,江苏 南京 210019;6.中国石化华东油气分公司勘探开发研究院,江苏 南京 210019;
7.大连海事大学,辽宁 大连 116026)

摘要：中国东部新生代断陷湖盆是重要的油气富集区,始新统页岩为主要烃源岩与页岩油气储层。尽管各湖盆沉积时代相近,但在岩相特征、湖水盐度及有机质丰度方面差异显著,页岩的有机质富集机制尚缺乏系统认识。本文选取渤海湾盆地的济阳坳陷、辽河坳陷、江汉盆地和南襄盆地为研究对象,综合分析岩相分类、矿物组成、元素与同位素特征,探讨在中国东部气候驱动下的陆相页岩沉积环境差异与有机质富集机制。结果表明,始新世东亚夏季风增强导致气候强烈波动,约40 Ma各湖盆普遍达到最大水深。气候的周期变化引起水体盐度规律性变化,形成层状灰岩/白云岩、钙质/白云质泥岩、长英质页岩、钙质/白云质页岩等多种细粒岩相类型。辽河坳陷以含泥方沸石微晶白云岩为特征,东营凹陷以灰质页岩为特点,南襄盆地则主要分布粉砂岩,江汉盆地以白云岩/泥质钙芒硝岩为主。湖水的盐度具有规律性区域分异特征,总体由北向南逐渐从咸水—半咸水转变为咸水至盐湖环境。湖水盐度及水体氧化还原状态控制有机质的形成与保存:湿热气候有利于生物繁殖和有机质输入,一般总有机碳(TOC)含量较高;而干旱气候导致的水体高盐度增强水体分层和底水缺氧程度,有利于有机质保存,TOC含量不一定高,但生烃转化率高。济阳坳陷页岩TOC含量较高(1.5%～4.5%),含油饱和度指数(OSI)为131 mg/g。江汉盆地与辽河坳陷页岩TOC含量较低(0～3%),辽河坳陷平均OSI为16 mg/g,而江汉盆地平均OSI达到159 mg/g,表明高盐度、强分层和良好保存条件形成的盐碱沉积环境可能是控制页岩油富集的关键因素。研究结果揭示了中国东部始新世断陷湖盆古气候、湖水盐度、沉积环境与有机质富集之间的耦合关系,为认识气候驱动下的陆相页岩油形成与富集机制提供了区域性的地质依据。

关键词：咸化湖盆;混积页岩;页岩岩相;有机质富集;氧化还原;古盐度;古气候;始新统
中图分类号：TE132 **文献标识码**：A

Lithofacies and organic matter enrichment mechanisms of Eocene mixed shales in saline lacustrine basins, eastern China

Tang Xuan[1,2], Yun Lu[3,4], He Xipeng[4,5], Gao Yuqiao[4,6], Liu Yang[7], Guan Ziheng[1,2], Zhou Futong[1,2], Chen Yiran[1,2], Yu Guangzhan[1,2], Zuo Peng[1,2]

*(1. School of Energy Resources, China University of Geosciences (Beijing), Beijing 100083, China;
2. Key Laboratory of Strategy Evaluation for Shale Gas Resources, Ministry of Natural Resources, Beijing 100083, China;
3. Sinopec Petroleum Exploration and Production Research Institute, Beijing 102206, China;
4. State Key Laboratory of Shale Oil and Gas Enrichment Mechanisms and Efficient Development, Beijing 102206, China;
5. Sinopec East China Oil & Gas Company, Nanjing, Jiangsu 210019, China;
6. Exploration and Development Research Institute, Sinopec East China Oil & Gas Company, Nanjing, Jiangsu 210019, China;
7. Dalian Maritime University, Dalian, Liaoning 116026, China)*

Abstract: The Cenozoic rift lacustrine basins in eastern China are important hydrocarbon accumulation regions, with Eocene shales serving as major source rocks and shale oil and gas reservoirs. Despite similar depositional ages, the lake basins show significant differences in lithofacies characteristics, lake-water salinity, and organic matter abundance; a systematic understanding of the mechanisms of organic matter enrichment in shale is still lacking. This study selected the Jiyang Depression and Liaohe Depression in the Bohai Bay Basin, the Jianghan Basin, and the

收稿日期：2026-03-11。
第一作者简介：唐玄(1979—),男,博士,教授,从事页岩油气地质评价研究。地址:北京市海淀区学院路29号,邮政编码:100083。E-mail:tangxuan@cugb.edu.cn
基金项目：国家自然科学基金“超临界CO_2与陆相干酪根-油-水体系的相互作用机理研究”(42372164)。

Nanxiang Basin as the research objects. Through integrated analyses of lithofacies classification, mineral composition, and elemental and isotopic characteristics, the differences in continental shale sedimentary environments and organic matter enrichment mechanisms under climate-driven conditions in eastern China were investigated. The results showed that the intensified East Asian summer monsoon during the Eocene caused strong climatic fluctuations, with all basins generally reaching their maximum lake depth around 40 Ma. Cyclic climatic changes caused regular variations in lake-water salinity and led to the development of multiple fine-grained lithofacies, including laminated limestone/dolostone, calcareous/dolomitic mudstone, felsic shale, and calcareous/dolomitic shale. The Liaohe Depression was characterized by muddy analcime microcrystalline dolostone, the Dongying Sag by calcareous shale, the Nanxiang Basin mainly by siltstone, and the Jianghan Basin by dolostone/argillaceous glauberite rocks. Lake-water salinity exhibited regular regional differentiation, generally showing a north-to-south transition from saline-brackish to saline and ultimately to salt-lake environments. Lake-water salinity and water-column redox conditions controlled the generation and preservation of organic matter: warm-humid climates favored biological reproduction and organic matter input, generally resulting in higher total organic carbon (TOC) contents; in contrast, high water salinity caused by arid climate enhanced water-column stratification and bottom-water anoxia, favoring organic matter preservation. Although TOC contents were not necessarily high, the hydrocarbon generation conversion rate was high. Shales in the Jiyang Depression had relatively high TOC contents (1.5%-4.5%) and an oil saturation index (OSI) of 131 mg/g. Shales in the Jianghan Basin and Liaohe Depression had lower TOC contents (0-3%); the Liaohe Depression had an average OSI of 16 mg/g, whereas the Jianghan Basin had an average OSI of 159 mg/g, indicating that saline - alkaline depositional environments formed under high salinity, strong stratification, and favorable preservation conditions may be a key factor controlling shale oil enrichment. The findings reveal a coupling relationship among paleoclimate, lake-water salinity, depositional environments, and organic matter enrichment in Eocene rift lacustrine basins of eastern China, providing a regional geological basis for understanding the formation and enrichment mechanisms of continental shale oil under climate-driven conditions.

Keywords: saline lacustrine basin; mixed shale; shale lithofacies; organic matter enrichment; redox; paleosalinity; paleoclimate; Eocene

目前，中国东部盆地是陆相页岩油勘探开发主战场[1-2]。相较于海洋沉积环境，湖泊环境对气候更为敏感，湖相页岩在干湿气候频繁交替和湖平面剧烈波动的背景下表现出非均质性强和黏土矿物含量高的特征，也给页岩油气资源的富集带来巨大影响[3-5]。在世界范围内，深湖环境生成的页岩油也占很大比例，典型的湖相页岩包括美国尤因塔盆地的绿河组，澳大利亚库珀盆地的罗斯尼思组、伊普西隆组和默特里组，巴基斯坦科哈特盆地的巴哈杜尔—凯尔组，印度阿萨姆—阿拉干盆地的科皮里组，以及中国茂名盆地油柑窝组、珠江口盆地文昌组、北部湾盆地流沙港组、依兰盆地达连河组、柴达木盆地的下干柴沟组、渤海湾盆地的沙河街组、江汉盆地的潜江组、南襄盆地的核桃园组。中国东部古近纪始新世发育了多套富有机质页岩，包括渤海湾盆地的沙河街组、江汉盆地的潜江组和南襄盆地的核桃园组。不同湖盆显示出不同的湖水盐度特征，进而在页岩有机物富集、油气生成和保存特征方面表现出较大差异，前人认识可能受到纬度、气候、海侵和火山的影响[6-7]。

目前研究表明：①对于始新统混合页岩岩相的研究已从单一矿物分类，发展到综合矿物组分、沉积构造和有机质丰度的多因素分类。例如，济阳坳陷始新统页岩被划分为4个大类、9个小类岩相[6]。②有机质富集受环境影响较大，影响要素包括生产力、保存条件、湖水盐度、水深等因素，有机质富集是高初级生产力和强还原保存条件共同作用的结果。咸化水体易形成盐度分层，底层缺氧利于有机质保存。但不同盆地有机质富集的主控因素存在差异[7-8]，例如柴达木盆地下干柴沟组上段因营养供给不足和沉积速率快，导致总有机碳（TOC）含量偏低[9]。③泥质纹层和灰质纹层通过控制黏土矿物转化和碱性矿物溶蚀-再沉淀对页岩生烃产生影响。目前，针对单个盆地或凹陷的案例分析较多，而针对古气候等具有广泛区域性影响的认识不足。亟待从更宏观的角度，系统性对比分析影响页岩沉积的核心参数，厘清参数的适用性条件，从而形成更科学的认识和结论。

以中国东部始新统咸化湖盆为研究对象（图1），以古新世—始新世极热期至始新世—渐新世过渡期等全球重大气候事件和东亚季风为背景，从古气候、古环境、古氧化还原条件和风化强度的角度，分析对比渤海湾盆地辽河坳陷、济阳坳陷的沙河街组三段（以下简称沙三段）至沙河街组四段（以下简称沙四段）、南襄盆地泌阳凹陷核桃园组三段（以下简称核三段）至核桃园组四段（以下简称核四段）、江汉盆地潜江凹陷潜江组二段（以下简称潜二段）至潜江组三段（以下简称潜三段）TOC含量和生烃潜力的差异，总结4个盆地始新统页岩有机质富集和生烃机制。所得结论具有广泛的推广价值，对东部盆地页岩新区块勘探和开发具有重要帮助。

1 地质与气候背景

1.1 地质背景

中国东部盆地古近系始新统湖相页岩分布广，从北向南依次为渤海湾盆地辽河坳陷沙河街组、渤海湾盆地

济阳坳陷沙河街组、南襄盆地泌阳凹陷核桃园组、江汉盆地潜江凹陷潜江组[10-13]。

辽河坳陷位于渤海湾盆地东北部，坳陷区处于断层控制下的新生代长期沉降带，以大幅度深陷为特征，古近系地层发育，具有良好的油气生成和储集条件[14]，发育多套湖相暗色泥岩。根据岩性、电性和生物组成特征，沙河街组自下而上可分为4个段，分别为沙四段、沙三段、沙河街组二段（以下简称沙二段）和沙河街组一段（以下简称沙一段）。以浅湖、半深湖相泥页岩及扇三角洲相砂砾岩、砂岩沉积为主，局部发育湖相碳酸盐岩。始新世中期沙三段沉积时期，辽河坳陷整体处于裂谷拉张深陷期，沉积了巨厚的半深湖—深湖相砂泥岩地层，页岩地层在西部凹陷、东部凹陷和大民屯凹陷广泛分布。

济阳坳陷在构造上属于渤海湾盆地中部次级负向构造单元，经历了多期构造运动，其构造演化过程可大致分为古生代挤压变形阶段、中生代的断陷阶段以及新生代的断裂拉张构造运动3个演化阶段，新生代是渤海湾盆地伸展裂陷的主要阶段。东营凹陷古近纪地层为煤和油页岩油等非常规能源矿产的重要赋存层位，主要页岩层段为沙三下亚段、沙四上亚段[15]。

南襄盆地形成于中生代，是位于新生代扬子地台与秦岭—大别造山带交汇发育的陆相断陷盆地。盆地可进一步划分为3个凹陷和4个凸起。凹陷即襄枣凹陷、南阳凹陷和泌阳凹陷；凸起包括新野凸起、师岗凸起、社旗凸起和唐河低凸起[16]。南襄盆地核桃园组经历了强烈断陷期，厚度介于2 000～3 000 m，可划分为三段：核三段为主力含油层系，该段厚度介于1 100～2 000 m，其下部和中部为深灰色泥岩夹白云岩和砂岩，上部为碱性白云岩；核桃园组二段（以下简称核二段）厚度介于700～800 m，岩性主要为泥质白云岩、白云质泥岩、泥岩和油页岩；核桃园组一段（以下简称核一段）厚度介于400～500 m，局部与下伏的大仓房地层呈不整合接触，岩性主要为灰绿色泥岩、白云岩和油页岩[17]。

江汉盆地是位于中扬子地块内的中新生代中型裂谷盆地[18]。盆地当前特征主要形成于晚侏罗世至早白垩世。由于中国东部的陆内造山运动，周围山脉带和地块经历了强烈的隆起[19-20]。从晚白垩世到古近纪，江汉盆地经历了太平洋板块回撤和南亚碰撞引起的上地幔活跃上涌。这种背景导致了多期裂谷作用，并在盆地中形成了广泛的硅质碎屑沉积物、蒸发岩和大量玄武岩流沉积物。江汉盆地包括十几个次级凹陷，其中潜江凹陷是位于盆地中部的富烃凹陷（图1）[10-13]。从晚白垩世到古近纪，潜江凹陷经历了2个不同的伸展裂谷阶段，以玄武岩熔岩流的多次幕式喷出为特征[18]。江陵凹陷古近系沉积序列中存在多种类型岩石，包括碎屑岩、碳酸盐岩、蒸发岩和油页岩[21]，在古新世至始新世早期，潜江凹陷受环境影响，岩性以蒸发岩为主[22]。

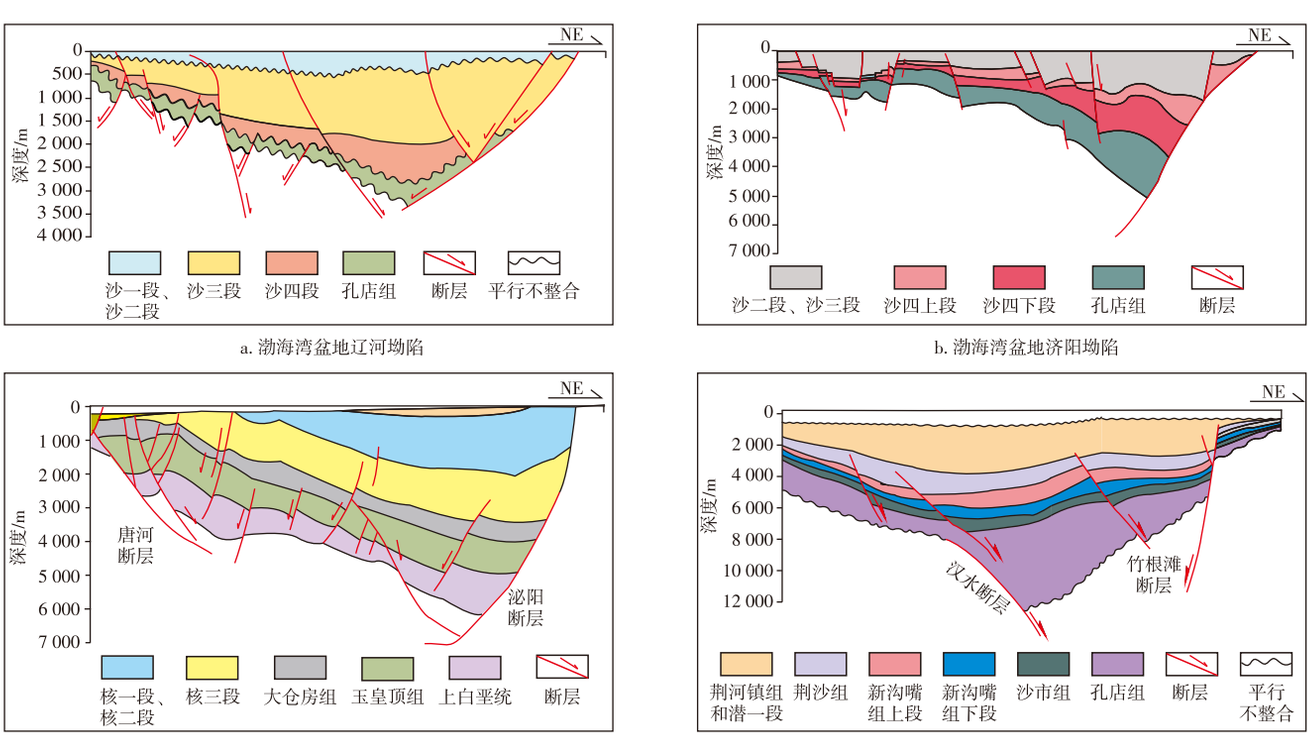

a. 渤海湾盆地辽河坳陷　　b. 渤海湾盆地济阳坳陷

c. 南襄盆地泌阳凹陷　　d. 江汉盆地潜江凹陷

图1　中国东部主要盆地构造背景（据文献[10-13]修改）

Fig. 1　Tectonic settings of major basins of eastern China (modified from references [10-13])

1.2 气候影响要素

1.2.1 东亚夏季风

始新世时期，亚洲东部是显著的季风影响区[23]。东亚季风主要受太阳辐射、大气环流及陆海热力差异等多重因素的综合控制，具有显著的大陆性、季节性和复杂性特征。结合前人花粉记录与古气候重建结果可知，在晚白垩世至古新世期间，中国存在一条自西向东延伸的广泛干旱带[24]，表明当时气候格局呈现出明显的干湿分带特征，东亚季风体系尚未形成或仍处于早期阶段。随后，中国东部地区在渐新世与中新世的分界期，气候由干旱转变为湿润。气候分带的基线变化通常被解释为全球大气环流格局由行星环流向季风环流转变的标志[25]。多项研究表明，东亚夏季风的盛行与加强，使来自海洋的水汽得以大规模输送至中国东部地区，从而显著增强了区域降水，推动了气候的湿润性[26]。这一过程不仅重塑了中国东部的古气候格局，也对沉积环境演化和有机质富集过程产生了深远影响。前人研究了氧同位素与东亚夏季风强度之间的关系，并利用济阳坳陷沙三段至沙四段氧同位素的纵向分布，明确了始新世期间中国东部广大地区东亚夏季风的变化趋势。

1.2.2 极热事件

始新世是地质历史的关键时期，发生了一系列全球气候事件，包括古新世—始新世极热事件（Paleocene-Eocene Thermal Maximum，PETM）、早始新世气候适宜期（Early Eocene Climatic Optimum，EECO）、中始新世气候适宜期（Middle Eocene Climatic Optimum，MECO）以及晚始新世—早渐新世全球气候变冷事件。研究表明，古近纪主要发生2次全球性的气候变化，分别为PETM和始新世—渐新世变冷事件。

PETM是巨量碳注入地球表层系统所导致的一次快速增温事件[27-30]，发生在距今55 Ma的始新世初，在一个地质年代时期内全球平均气温上升5～8 ℃，陆地生态系统的初级生产力在PETM事件后得到大幅提升。虽然历时短暂，只有约200 ka [31-32]，地球温暖时间持续了80～200 ka，但对整个始新世的气温都产生了巨大影响，整个始新世期间直到渐新世都是偏温暖的气候。

发生PETM后，始新世期间又发生了2次极热事件，即EECO和MECO。PETM和第二次始新世极热事件（Eocene Thermal Maximum 2，ETM-2）为短周期的极热事件，持续时间介于10～200 ka；EECO和MECO为长周期极热事件，但每个独立的热事件持续时间较短[23-24,27]。始新世—渐新世过渡期（Eocene-Oligocene transition，EOT）发生在34 Ma前后，是新生代最显著的气候变冷事件之一，标志着地球气候由“温室”进入“冰室”[33]。中始新世气候最适宜期，即MECO是在40 Ma前发生持续时间约500 ka的广泛海洋-大气变暖事件，主要表现为大气CO_2含量上升、生物变化和深海碳酸盐溶解时间延长[34-36]。

1.2.3 火山活动

渤海湾盆地辽河坳陷沙三段和江汉盆地潜江凹陷潜三段、潜江组四段（以下简称潜四段）发现了火山活动的痕迹。火山喷发会释放大量的SO_2与火山灰。SO_2在大气中转化形成酸雨，加速了陆源物质的风化，从而增强了陆源碎屑及营养物质向湖泊体系的输入。与此同时，火山灰的分解也可释放出丰富的营养元素，为湖泊沉积体系提供了额外的物质来源。这2种途径所提供的丰富营养物质显著提升了湖盆的初级生产力，促进了有机质的沉积与富集。在研究区江汉盆地潜江凹陷地区，火山灰沉降释放的营养元素进一步促进了湖盆的生物繁盛，但随之而来的高温与盐度升高的环境条件，也可能对水生生物的生长造成一定限制。

1.2.4 海侵事件

始新世时期，中国东部多个盆地受到不同程度的海侵影响，例如研究区中渤海湾盆地济阳坳陷以东地区[37-43]，已有研究认为海侵过程有利于湖盆中优质烃源岩的形成与保存[44-46]，其主要机制包括：①海水的侵入携带丰富的营养物质，提升了湖泊初级生产力；②海侵增强了湖水分层，使深水区氧气补给受限，从而导致底层水体的氧化还原条件发生变化，有助于有机质的富集与保存[47-48]。

济阳坳陷沙四段上部发生海侵的证据是发现大量各种海相和海陆过渡相化石，沙三段下部主要包括大量各种孔虫和甲藻的海相化石，表明在渤海湾盆地中最富油气的烃源岩层段，即沙三段、沙四段受到海洋影响。这些层段的烃源岩被认为比纯湖相层段烃源岩具有更高的TOC含量（≥2%）和更优质的有机质类型（Ⅰ型或Ⅱ型干酪根）[44-45]。济阳坳陷在海水侵入时期形成的烃源岩含有丰富的藿烷，TOC含量大于2%，S_1+S_2（S_1为游离烃的含烃量，S_2为裂解烃的含烃量，S_1+S_2用来表示生烃潜量）含量为20 mg/g[44-45]。泌阳凹陷核三段通过古生物学、微量元素和生物标志物被证实有海侵现象发生[43]。

1.2.5 CO_2含量变化

总体来看，始新世期间大气CO_2含量呈先升后降的变化趋势，其转折点出现在EECO。从EECO至晚EOT，CO_2含量总体处于持续下降阶段，仅在MECO出现短暂回升。东亚夏季风强度的变化趋势与CO_2含量具有良好

对应关系，同样表现为先增强后减弱的特征，其转折期也与MECO时期对应。全球大气CO_2含量的波动及东亚夏季风强度的演化与始新世关键气候事件密切相关，大气中CO_2含量升高也可能和EECO高温加速了硅酸盐风化有关[49]，形成了足够厚的碳酸钠蒸发岩所需碱性较高的水体条件，这种条件下的化学风化作用增强解释了美国和中国在始新世时期碳酸钠蒸发岩群的形成过程[50]。

2　方法与数据来源

本文以中国东部盆地典型断陷咸化湖盆为研究对象，结合始新世时期中国东部的沉积构造背景和气候变化背景，对渤海湾盆地辽河坳陷和济阳坳陷沙三段—沙四段、南襄盆地泌阳凹陷核二段—核三段和江汉盆地潜江凹陷潜三段—潜四段的陆相页岩开展岩相、矿物、有机质和古气候比较研究。开展典型井分析，包括X射线衍射分析矿物组成、X射线荧光光谱法元素分析、碳氧同位素分析、TOC含量和岩石热解分析，并结合大量前人研究结果，系统分析中国东部盆地页岩岩相和元素组成的纵向变化，依据元素变化探究始新世时期古气候变化，以及古气候对古环境、有机质富集和生烃的影响，最后形成始新世时期中国东部地区咸化湖盆形成模式。

3　页岩岩相与元素组成

3.1　矿物成分和岩相

渤海湾盆地辽河坳陷沙三段至沙四段的矿物主要由碳酸盐矿物和黏土矿物组成，黏土矿物含量介于50%～100%，碳酸盐矿物含量介于50%～100%，长英质矿物含量介于25%～75%（图2）[51-54]，碳酸盐矿物包括方解石、白云石和方沸石。渤海湾盆地济阳坳陷沙三段至沙四段矿物主要由碳酸盐矿物和长英质矿物组成，碳酸盐矿物含量介于50%～100%，长英质矿物含量介于50%～100%，黏土矿物含量介于20%～80%。南襄盆地泌阳凹陷核桃园组中，矿物成分包括碳酸盐矿物、长英质矿物和黏土矿物。碳酸盐矿物包括方解石、白云石和方沸石。江汉盆地潜江凹陷潜江组的矿物成分主要集中在高碳酸盐岩含量（50%～100%）、高硅酸盐岩含量（75%～100%）和相对较低的黏土矿物含量，碳酸盐矿物包括方解石和白云石。

4个研究区始新统页岩都包含混合岩相。碳酸盐矿物含量高的区域与盐湖有关。除混合岩相区分布外，渤海湾盆地济阳坳陷沙三段至沙四段和江汉盆地潜江凹陷潜江组也分布在碳酸盐矿物含量高的地区，渤海湾盆地辽河坳陷的沙三段至沙四段则分布在黏土矿物含量高的地区。

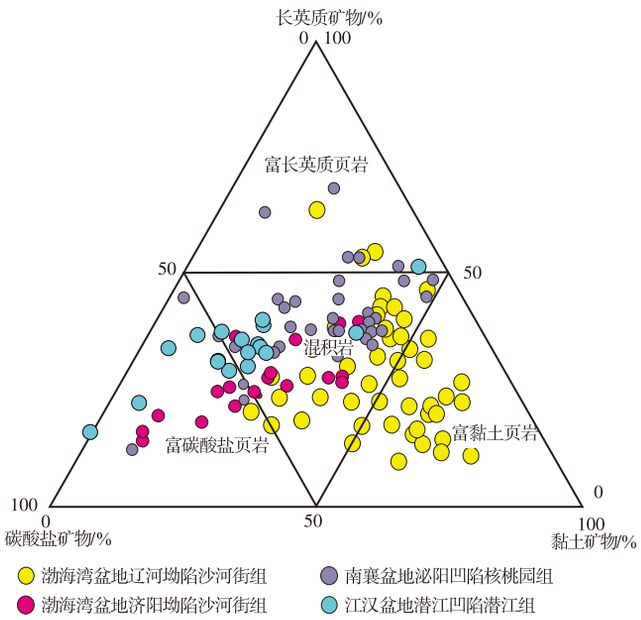

图2　中国东部盆地始新统页岩矿物组成（据文献[51-54]修改）

Fig. 2　Mineral composition of Eocene shale in basins of eastern China (modified from references [51-54])

从北到南，黏土矿物含量逐渐降低，硅质矿物含量逐渐增加。从岩相组成来看，渤海湾盆地辽河坳陷沙三段至沙四段的页岩岩相包括泥质页岩、混合岩性页岩、粉砂质混合页岩和钙质混合页岩[55-57]。渤海湾盆地济阳坳陷沙三段至沙四段的岩相组成包括层状灰岩、互层灰岩、层状黏土岩、层状细粉砂岩、层状泥质细粒混积岩和层状粉质黏土细粒混积岩。南襄盆地泌阳凹陷核三段的岩相包括块状硅质泥岩、块状泥质页岩、层状砂质页岩、层状黏土质页岩、层状钙质页岩、层状泥质页岩和砂岩[17]。江汉盆地潜江凹陷的潜三段至潜四段岩相包括灰色泥质石膏、灰色泥岩、浊/钙质石膏、浊混积岩、灰色混积岩、泥质混积岩、硫酸盐混积岩和盐岩[58-61]。

4个研究区在始新统页岩层段均有泥页岩、灰质页岩、云质页岩，济阳坳陷还包括粉砂岩、灰岩，泌阳凹陷还包括粉砂岩，潜江凹陷还包括云岩、钙芒硝岩和石盐岩。从北往南，咸化程度逐渐增强，从咸水—半咸水逐渐转化为咸水至盐湖环境（图3）。

3.2　主、微量元素分布

在湖泊沉积物中，通常使用主、微量元素分布来指示古沉积环境，包括古盐度、古氧化还原条件、古气候等（表1）[62-65]。通过运用对沉积环境反应敏感的Sr、Ba、Cu、Mn、Ca、Ni、V、Th、U、Ti、Mg等元素，结合相应的主、微量元素参数比值对中国东部盆地典型页岩层系（渤海湾盆

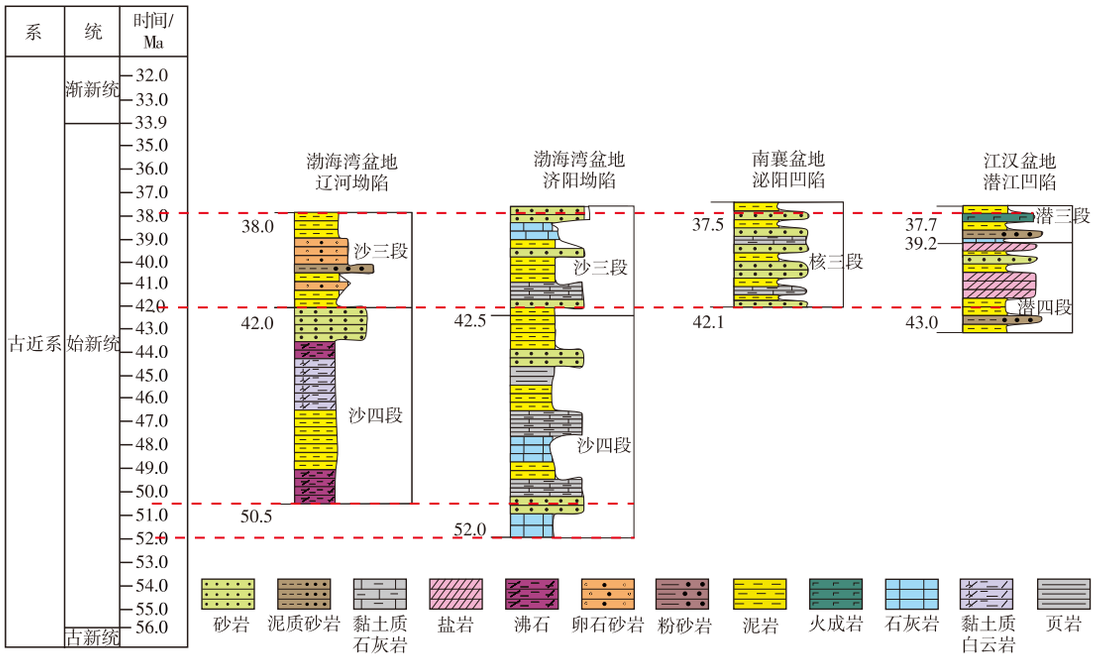

图3　中国东部古近系页岩对比（据文献[58-61]修改）

Fig. 3　Comparison of Eocene shale column, East China (modified from references [58-61])

表1　沉积古环境判识参数指标（据文献[62-65]修改）

Table 1　Paleosedimentary environmental parameter indicators (modified from references [62-65])

参数类型	参数指标	参数划分		
		淡水湖相	微咸湖相	咸湖相
古盐度	$\omega(Sr)/\omega(Ba)$	<0.2	0.2～0.5	>0.5
	$\omega(CaO)/[\omega(CaO)+\omega(Fe)]$	<0.2	0.2～0.5	>0.5
	$1\,000\,\omega(Rb)/\omega(K)$	<4.0	4.0～6.0	>6.0
	$\omega(B)/\omega(Ga)$	<3.0	3.0～6.0	>6.0
参数类型	参数指标	参数划分		
		气候温暖湿润	气候半湿润	气候干燥炎热
古气候	$\omega(Sr)/\omega(Cu)$	<5.0	5.0～10.0	>10.0
	气候指数（C）	>0.8	0.2～0.8	<0.2
参数类型	参数指标	参数划分		
		氧化环境	贫氧环境	还原环境
古氧化还原	$\omega(Ni)/\omega(Co)$	<5.00	5.00～7.00	>7.00
	$\omega(U)/\omega(Th)$	<0.75	0.75～1.25	>1.25
	$\omega(V)/\omega(Cr)$	<2.00	2.00～4.25	>4.25

地辽河坳陷沙河街组、渤海湾盆地济阳坳陷沙河街组、南襄盆地泌阳凹陷核桃园组和江汉盆地潜江凹陷潜江组）形成的古环境进行综合研究。

在古盐度方面，常用的参数有$\omega(CaO)/[\omega(CaO)+\omega(Fe)]$、$\omega(Sr)/\omega(Ba)$、$1\,000\,\omega(Rb)/\omega(K)$和$\omega(B)/\omega(Ga)$[48]。在天然水中，Sr元素在相同条件下比Ba元素运移更远。在淡水与盐水混合时，淡水中的Ba^{2+}会与盐水中的SO_4^{2-}结合形成$BaSO_4$，然后发生沉淀。$SrSO_4$具有很高的溶解度，在生物作用下发生进一步运移和沉淀[60-62, 66-67]。Ba和Sr在岩石埋藏成岩过程中会发生显著改变，一些含Sr矿物会在成岩作用过程中释放出Sr^{2+}，如长石的钠长石化和蒙脱石的脱水过程[68]。此外，Ba在埋藏成岩过程中也很容易迁移[69-70]。在成岩作用的早期阶段，富含有机质的沉积物中通常含有大量的重晶石，这些重晶石在缺氧的底层水或孔隙水中发生还原性溶解[71]，导致了Ba^{2+}的释放[17]。

在古氧化还原方面，$\omega(V)/[\omega(V)+\omega(Ni)]$、$\omega(Ni)/\omega(Co)$和$\omega(V)/\omega(Ni)$常被作为恢复古水体氧化还原条件的地球化学指标。在氧化环境中，Ni以Ni^{+}的形式存在，而Co以Co^{2+}的形式溶解在水中。古氧化还原条件反映了沉积期湖水的含氧量。V、Ni和Cr对沉积环境中的氧化还原变化很敏感，能够反映古环境的氧化还原条件[72-73]。$\omega(V)/[\omega(V)+\omega(Ni)]$值大于0.84，表明水体分

层，底层水中存在H_2S厌氧环境；$\omega(V)/[\omega(V)+\omega(Ni)]$值介于0.54～0.72，表示水体分层不明显的厌氧环境；$\omega(V)/[\omega(V)+\omega(Ni)]$值介于0.46～0.60，表示水体弱分层的贫氧环境[74]。

古气候影响水位变化和水环境条件。古温度、湿度和日照量控制着碳酸盐种类的多样性、生成量和沉积过程。此外，温暖的气候条件往往能提供充足的降雨，使河流能够将营养物质和有机质输送到湖泊，从而进一步提高初级生产力[75]；然而也会导致水分层和流动循环弱。在古气候方面，气候指数（C）和古盐度恢复采用$\omega(Sr)/\omega(Cu)$，其中$C=\sum[\omega(Fe)、\omega(Mn)、\omega(Cr)、\omega(Ni)、\omega(V)、\omega(Co)]/\sum[\omega(Ca)、\omega(Mg)、\omega(K)、\omega(Na)、\omega(Sr)、\omega(Ba)]$，Sr是喜干元素，Cu是喜湿元素。在干旱条件下，由于供水减少和水质碱度增加，Ca、Mg、K、Na、Sr、Ba等元素大量沉淀和沉积；在潮湿的气候条件下，岩石中存在更多的元素，如Fe、Mn、Cr、Ni、V、Co。

通常在温暖潮湿的条件下，降雨量充足；而在干旱条件下，淡水输入减少和蒸发强度提高会导致湖水盐含量增加，可能会增加$\omega(Mg)/\omega(Ca)$值，并随后导致碳酸盐（白云石）的沉淀。因此，较高的$\omega(Mg)/\omega(Ca)$值表示在干燥气候条件下水分蒸发强度更高[17]。

Nesbitt等[63]首次提出了化学蚀变指数（CIA）来定量评估沉积岩（泥岩）的风化历史，用于评估泥质岩的化学风化强度与物源区风化历史[64-65, 76-79]。该指标的理论基础在于化学风化过程中长石类矿物的分解及其向黏土矿物的转化过程。

$$I_{CIA}=\{\chi(Al_2O_3)/[\chi(Al_2O_3)+\chi(CaO)+\chi(Na_2O)+\chi(K_2O)]\}\times 100 \quad (1)$$

式中：I_{CIA}为化学蚀变指数；$\chi()$表示摩尔分数。

CIA常用于表征源区化学风化强度：CIA介于50～<65表示初级风化作用，65～85表示中等程度风化，而>85～100则反映了强烈化学风化过程。另外，CIA并非单纯反映化学风化程度，还可能受到多种因素的影响，包括沉积物物源差异、水动力条件下的粒度分选效应以及沉积后期K^+的加入（如成岩伊利石化或交代作用）。在富含碳酸盐的泥质岩中直接采用CIA评估风化强度可能导致偏差，因为碳酸盐矿物中的CaO会干扰硅酸盐系统中CaO摩尔分数计算，从而降低指数的准确性[80-82]。

4　气候对沉积环境的影响

从始新世早期开始，4个盆地的湖水都具有较高的盐度，这与盆地的干热气候有关。在干旱气候的影响下，古湖水不断蒸发浓缩，在凹陷内形成了咸水沉积体系。江汉盆地盐度较高，渤海湾盆地次之。江汉盆地潜江组具有碳酸钙和盐岩等特征性盐湖矿物，而渤海湾盆地辽河坳陷具有石膏等特征性盐湖矿物。渤海湾盆地在始新世早期至47 Ma的盐度相对较高，47 Ma之后到始新世末期表现出微咸水的特征。在古气候方面，这4个地区在始新世期间均表现为干热气候，而渤海湾盆地的气候在47～45 Ma期间经历了从干旱到湿润、半湿润的转变。东营凹陷和泌阳凹陷的$\omega(Sr)/\omega(Cu)$值相对较小，反映了相较于辽河坳陷和潜江凹陷更湿润的气候，而潜江凹陷则处于干热气候中（图4）[12, 83]。在页岩发育区间内，Sr、B、V元素在泌阳凹陷核三段下部相对富集较多，$\omega(Sr)/\omega(Cu)$值普遍大于10，$\omega(V)/\omega(Cr)$值普遍大于2，反映了这个时期主要为干热气候，沉积环境为微还原的咸水环境；核三段的上部与下部相反，Sr、B和V元素含量显著降低（图5、图6）[12, 83-89]。$\omega(Sr)/\omega(Cu)$值一般小于10，$\omega(V)/\omega(Cr)$值

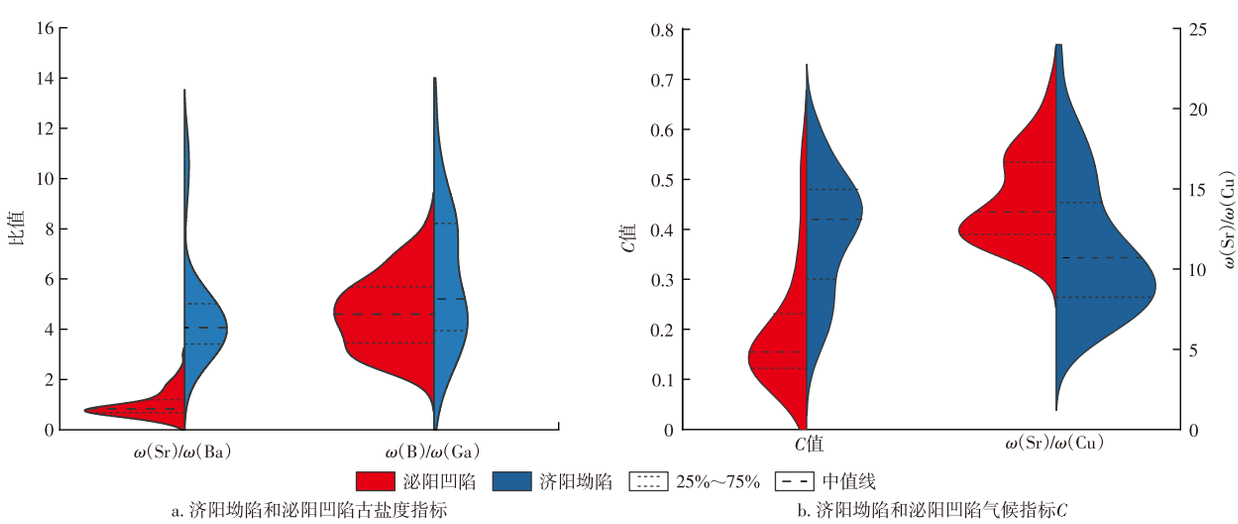

图4　济阳坳陷和泌阳凹陷古环境指标比较（据文献[12,83]修改）

Fig. 4　Comparison of paleoenvironment between Jiyang Depression and Biyang Sag (modified from references [12, 83])

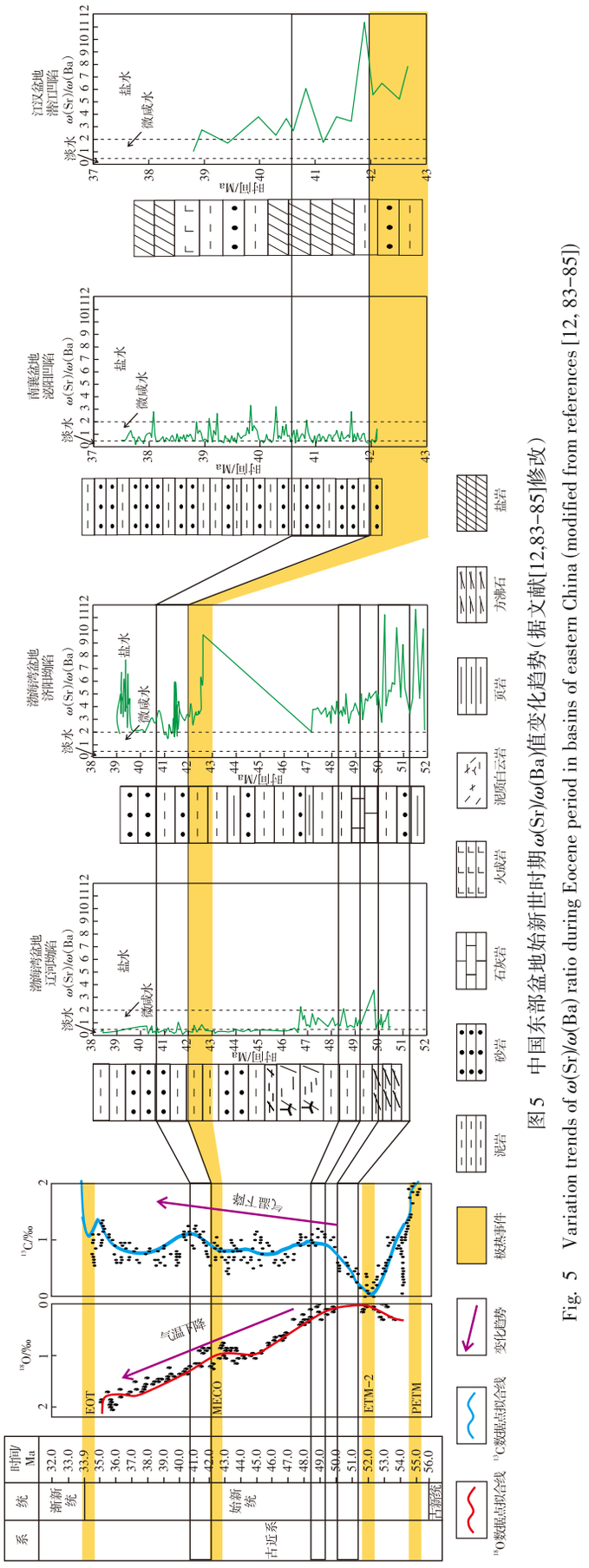

图5 中国东部盆地始新世时期$\omega(Sr)/\omega(Ba)$值变化趋势(据文献[12,83-85]修改)

Fig. 5 Variation trends of $\omega(Sr)/\omega(Ba)$ ratio during Eocene period in basins of eastern China (modified from references [12, 83-85])

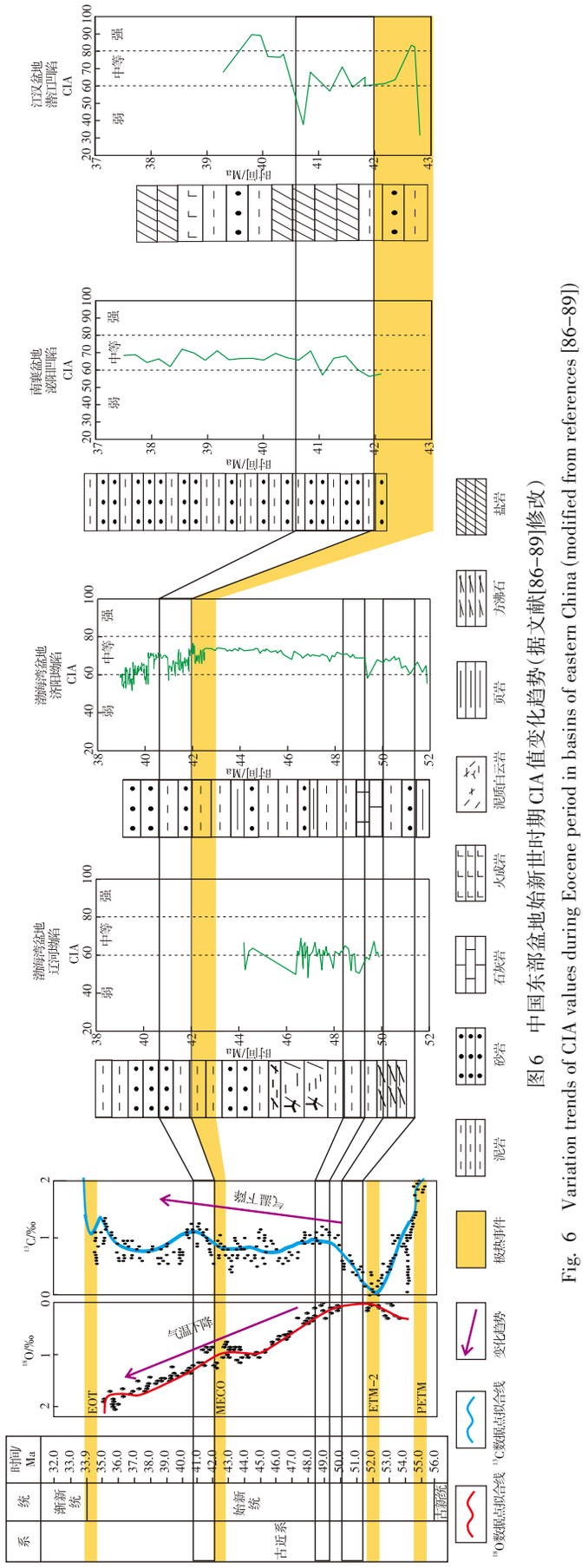

图6 中国东部盆地始新世时期CIA值变化趋势(据文献[86-89]修改)

Fig. 6 Variation trends of CIA values during Eocene period in basins of eastern China (modified from references [86-89])

大多小于2，表明气候主要为温暖湿润。潜四段沉积期，古气候指标中的化学蚀变指数小于0.2，ω(Sr)/ω(Cu)值极高，表明干热气候；潜三段沉积期ω(Sr)/ω(Cu)值下降，表明气候向温暖湿润开始转变(图7)[58-60, 90]。

在古氧化还原条件方面，40 Ma前后，4个盆地均表现出由还原环境向氧化环境过渡的趋势(图8)[85-87, 91]。从氧化-还原的角度来看，潜江凹陷的ω(V)/[ω(V)+ω(Ni)]值最高，均处于还原环境，而泌阳凹陷的ω(V)/[ω(V)+ω(Ni)]值最小，大多是在强氧化条件下。核三段下部的V元素相对富集，ω(V)/ω(Cr)值普遍大于2，表明该时期的沉积环境是一个相对还原的咸化环境；核三段上部与下部相反，V元素含量显著降低，ω(V)/ω(Cr)值大多小于2，表明沉积环境是弱氧化的淡水环境。52～47 Ma时期，风化程度逐渐增强，这与始新世早期全球气温的短暂上升有关。经过一段时间后风化程度开始减弱，在42 Ma左右再次增强。在这4个研究区中，辽河坳陷始新世的风化程度最弱，大部分时期属于弱风化。东营凹陷和潜江凹陷的风化程度较强，东营凹陷最强，这与古盐度参数Sr/Ba的趋势相似(图9)[58-60, 70, 78-80, 85-90, 92-93]。在岩性方面，4个地区的岩性在垂向上自下而上表现出砂泥比逐渐增大的趋势，由深湖的纯泥岩转变为半深湖的含砂质夹层泥岩。在40 Ma左右的MECO事件中，存在较厚的砂岩夹层，砂泥比显著增加。气候变热后，沉积速率呈增加趋势，季节差异变大，夏季降雨量增加，导致河流等来源的陆源碎屑输入增加，同时也提高了湖泊的生产力。

碳氧同位素是湖泊开放程度的良好指标。因为湖泊中的藻类会消耗^{12}C，从而增加水中的$\delta^{13}C$，而有机质的氧化会产生$^{12}CO_2$，导致水中$\delta^{13}C$减少。此外，淡水的$\delta^{13}C$远低于湖水，淡水流入会降低湖水的$\delta^{13}C$，而蒸发会增加湖水的$\delta^{13}C$[94]。在氧同位素中，较轻的^{16}O更有可能从水面逃逸到空气中，增加湖水的$\delta^{18}O$，而潮湿的气候和降雨将使湖水的$\delta^{18}O$接近淡水中通常记录的值[95]。根据研究结果整合了已发表的碳氧同位素数据(图9)[58-60, 70, 78-80, 85-90, 92-93]，在现代开放/封闭湖泊中通过同位素研究建立开放/封闭湖泊图解[96-97]。

非碱性微咸水湖是指在大多数时期水体盐度已达到碳酸盐饱和，但未达到硫酸盐和氯化物饱和的湖泊。非碱性咸水湖的典型例子包括始新世—渐新世渤海湾盆地(沙河街组沉积时期)东营凹陷[98-100]和松辽盆地(嫩江组和青山口组沉积时期)[101-103]的湖泊。碱性微咸水湖是指水体碱度高(pH值大于9)、矿化度相对较低、碳酸钠矿物欠饱和的湖泊。

根据含白云岩层序中是否存在丰富的同时代火山岩和凝灰质岩，中国碱性微咸水湖分为富凝灰岩型和贫凝灰岩型两种类型。两种碱性微咸水湖的白云岩由相似的碳氧同位素组成，表明其白云岩在成因上是有联系的。碱性微咸水湖白云岩的$\delta^{13}C$值为正，介于>0～10‰[104]，而其$\delta^{18}O$值大多为负，介于-20‰～<0[105-113](图10)[114-118]。渤海湾盆地辽河坳陷在古近系沙河街组沉积期间为贫凝灰岩型碱性微咸水湖[108]。碱性微咸水湖泊中的白云岩主要赋存于湖中心沉积物中，包括纹层状方沸石白云岩、钠长石白云岩、白云质方沸石、泥质白云岩和白云质泥岩等岩相。除了方沸石外，钠长石、重晶石和地开石在这些碱性微咸水湖沉积物中也很常见[106]。

碱性盐湖被称为“苏打湖”，其特征是在湖中心广泛沉积层状碳酸钠。中国碱性盐湖包括核桃园组沉积期的南襄盆地泌阳凹陷[104]。准噶尔盆地玛湖凹陷碱性盐湖与泌阳凹陷不同，还含有丰富的火山岩和凝灰岩物质[119]。碱性盐湖中的白云石矿物主要以孤立分散的晶体或聚集体赋存于白云质泥岩和白云质凝灰岩中[120-121]。碱性盐湖白云岩的$\delta^{13}C$值介于0～7‰，$\delta^{18}O$值介于5‰～15‰[119, 121-124](图10)。

根据4个凹陷碳氧同位素的平面分布来看，渤海湾盆地辽河坳陷沙三段至沙四段水体为碱性微咸水湖，渤海湾盆地东营凹陷沙三段至沙四段水体为非碱性盐湖和碱性咸化湖泊，南襄盆地泌阳凹陷核一段至核二段水体为碱性盐湖，江汉盆地潜江凹陷潜三段至潜四段水体为非碱性咸湖。

5 气候对有机质富集及含油性的影响

渤海湾盆地辽河坳陷烃源岩TOC含量相对较低，主要集中在0～3%，表现出明显的两段式分布特征。第一阶段为42.4～39.2 Ma，有机质富集程度最高时间在42.0 Ma左右(TOC含量为2.5%)；第二阶段为39.1～38.0 Ma，有机质富集峰值在38.5 Ma左右(TOC含量为2.8%)。渤海湾盆地东营凹陷沙三段页岩的TOC含量主要分布在1.5%～4.5%，有机质含量普遍较高。从下到上，表现为2个长期变化阶段。第一阶段为42.4～39.2 Ma，有机质富集度最高时间在41 Ma左右(TOC含量为4.5%)；第二阶段为39.1～38.0 Ma，有机质富集度出现峰值时间在38.5 Ma左右(TOC含量为3.0%)。南襄盆地泌阳凹陷核三段TOC含量相对较高，主要分布在0～6%，在42.1～37.5 Ma呈现出波动增加的趋势，在39.2～38 Ma处于大规模有机质富集阶段，TOC含量主要分布在2%～6%。江汉盆地潜江凹陷烃源岩TOC含量也相对较低，主要分布在0～4%，整体表现出较大的波动，在40.2 Ma时达到最大值3.8%(图11)[60, 92-93, 125]。4个研究区页岩的有机质类型都以Ⅰ型和$Ⅱ_1$型为主，为生油型有机质[126-129]。

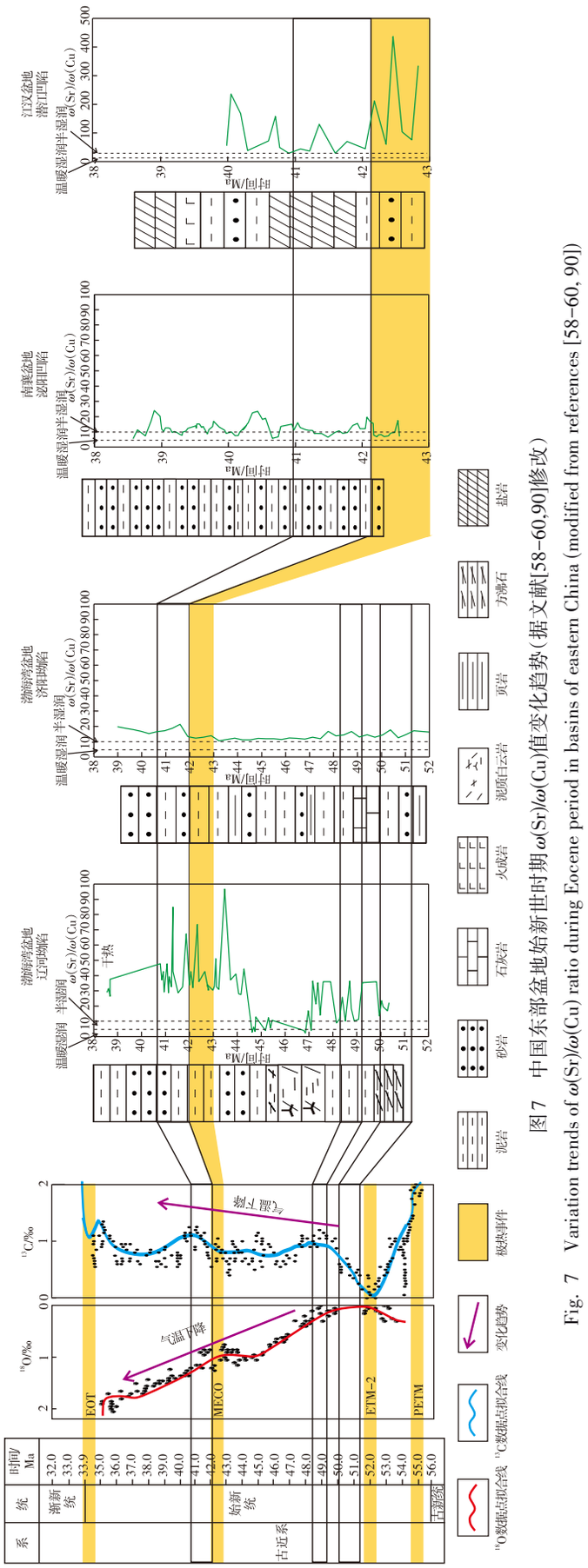

图7 中国东部盆地始新世时期ω(Sr)/ω(Cu)值变化趋势(据文献[58-60,90]修改)

Fig. 7 Variation trends of ω(Sr)/ω(Cu) ratio during Eocene period in basins of eastern China (modified from references [58-60, 90])

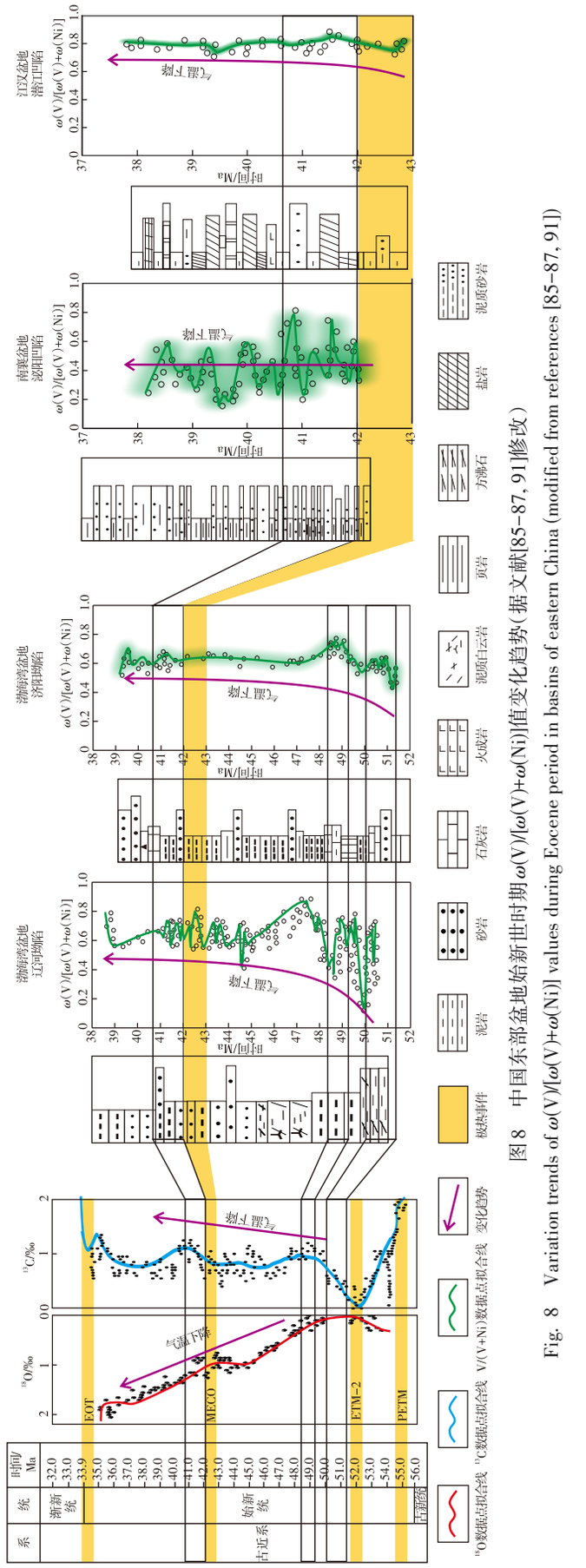

图8 中国东部盆地始新世时期ω(V)/[ω(V)+ω(Ni)]值变化趋势(据文献[85-87, 91]修改)

Fig. 8 Variation trends of ω(V)/[ω(V)+ω(Ni)] values during Eocene period in basins of eastern China (modified from references [85-87, 91])

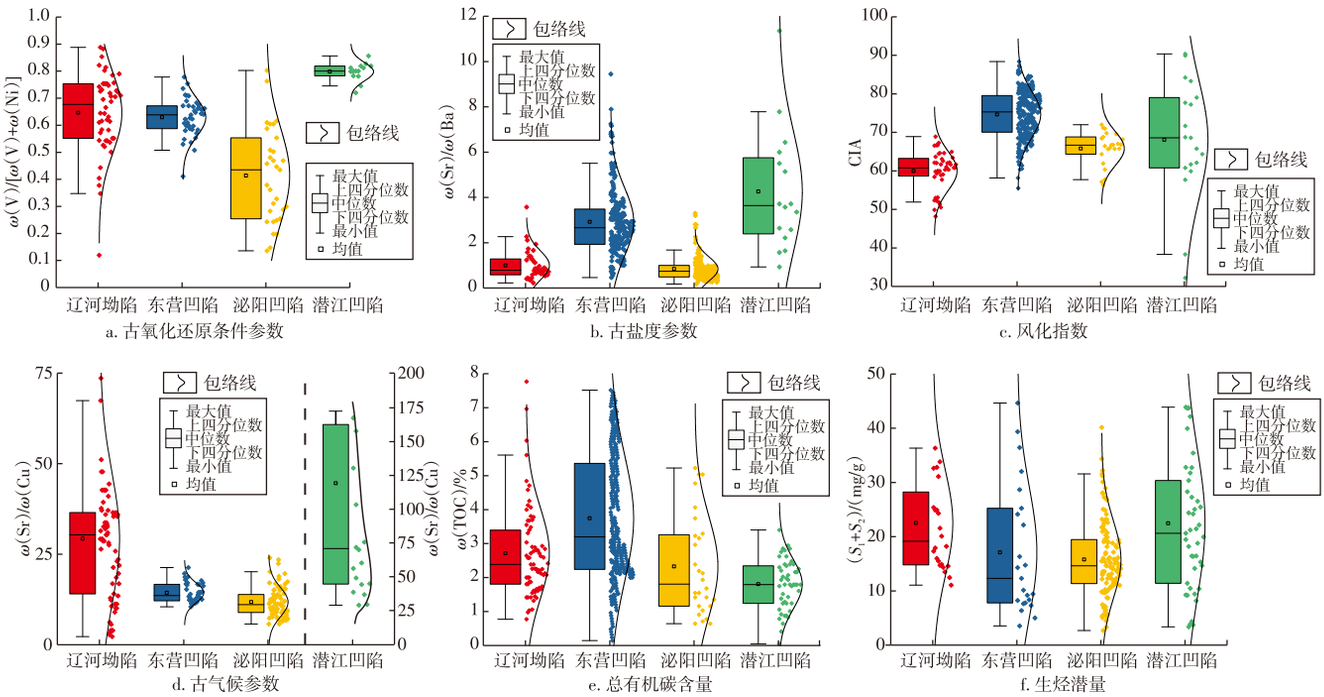

注：图9d潜江凹陷的$\omega(Sr)/\omega(Cu)$值见右侧纵坐标。

图9　中国东部区域始新统页岩地球化学参数箱线图（据文献[58-60, 70, 78-80, 85-90, 92-93]修改）

Fig. 9　Box plots of geochemical parameters of Eocene shale in eastern China (modified from references [58-60, 70, 78-80, 85-90, 92-93])

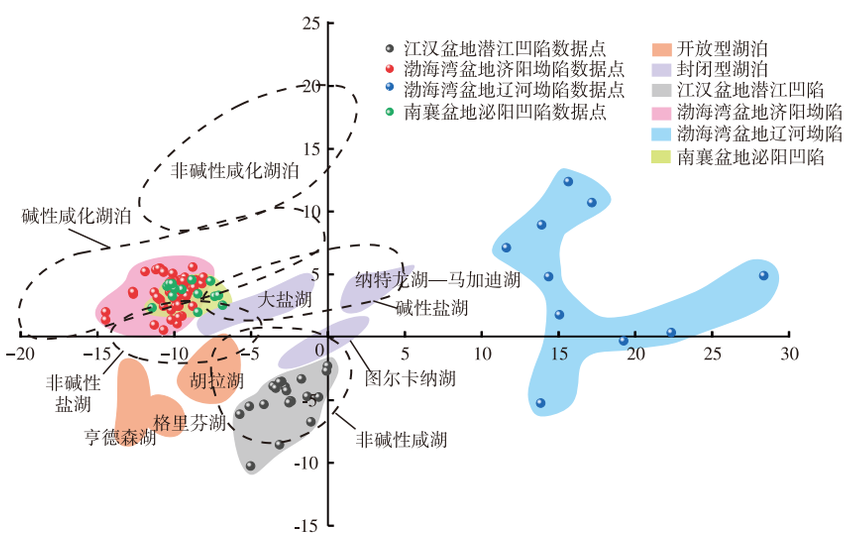

注：横坐标为$\delta^{18}O$, ‰；纵坐标为$\delta^{13}C$, ‰。

图10　湖盆类型划分（据文献[114-118]修改）

Fig. 10　Classification of lake basin types (modified from references [114-118])

在4个地区的始新统页岩中，从下到上总有机碳含量逐渐降低，对应大约55 Ma前PETM导致的全球变暖向大约34 Ma前EOT导致全球变冷的转变。全球气温升高会增强风化，温暖的气候有利于生物繁殖，使有机质来源更丰富。中始新世气候适宜期（MECO）发生在大约40 Ma前，全球气温短暂上升，41～39 Ma前，4个地区均有TOC明显短暂上升的现象。

横向对比4个盆地的TOC含量，渤海湾盆地辽河坳陷沙三段、沙四段的TOC含量最低，江汉盆地潜三段—潜四段的TOC含量也很低，南襄盆地核桃园三段的TOC含量相对较高。古盐度高的地区TOC含量较低，这可能与盐作为催化剂促进有机质热演化过程有关。同时，盐可以隔离有机质与氧气的接触，有利于有机质的保存。

综合比较4个研究区的TOC和S_1+S_2含量，东营凹陷是济阳坳陷的次一级凹陷，其TOC含量最高，但S_1+S_2的平均值和中值最低，反映了渤海湾盆地东营凹陷的生烃转化率较低。南襄盆地泌阳凹陷TOC含量排第二，但

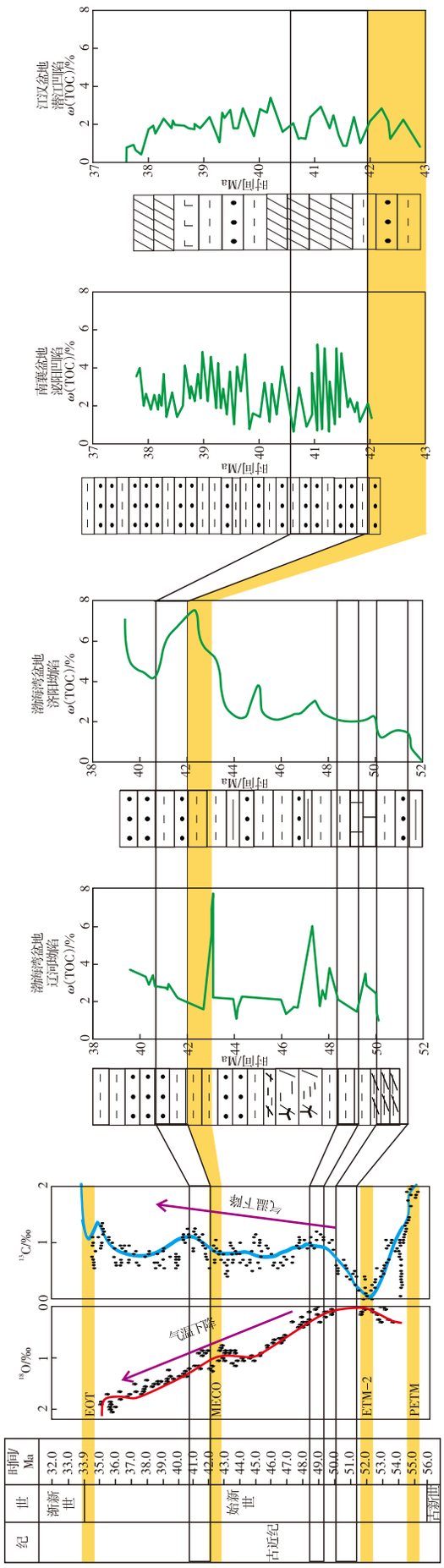

图11 中国东部盆地始新世时期TOC含量变化趋势(据文献[60, 92–93, 125]修改)

Fig. 11 Variation trends of total organic carbon (TOC) content during Eocene period in basins of eastern China (modified from references [60, 92–93, 125])

S_1+S_2含量较低，也具有生烃转化率低的特点。辽河坳陷和潜江凹陷具有相反的特征，TOC含量较低，但S_1+S_2含量较高，反映了这2个地区的高油气转化率（图12）[130-134]，这一现象可能与海侵作用将更多有机质输入到济阳坳陷和泌阳凹陷中有关。其中，济阳坳陷距离海洋较近，有机质输送更多。济阳坳陷和泌阳凹陷都具有相对潮湿的环境，有利于微生物生长，有机质分解作用更强，不利于有机质转化为油气，导致生烃转化率较低。

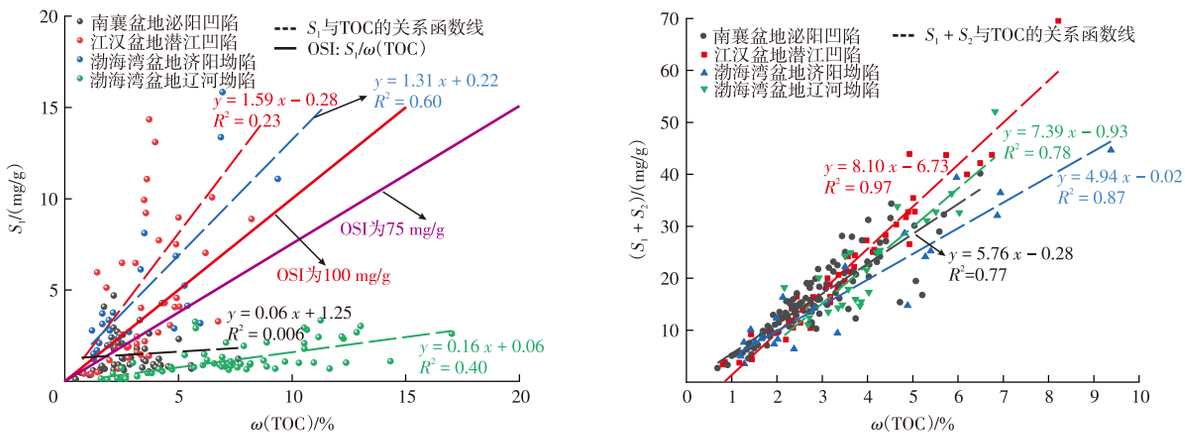

a. 中国东部盆地始新统页岩油的可动性　　b. 中国东部盆地始新统页岩油的含油量

注：OSI为含油饱和度指数。

图12　中国东部盆地始新统页岩油的可动性和含油量（据文献[130-134]修改）

Fig. 12　Oil mobility and content of Eocene shales in basins of eastern China (modified from references [130-134])

在有机质聚集后的早期成岩阶段，有机物发生强烈降解作用的同时，火山活动的影响使湖水中形成了缺氧-富硫化氢的水化学环境，从而改善了有机质的运移与保存条件，有利于优质烃源岩的形成[135]。前人研究认为，火山活动增强了陆源物质的风化作用，加速了风化产物的搬运与输入，从而导致进入湖泊的碎屑物质显著增加。与此同时，火山活动可能诱发湖盆内生物生产力的短期爆发，使黑色页岩在高生产力条件下沉积。火山喷发过程还会消耗环境中的氧气，使湖盆水体处于缺氧-富硫化氢环境，有利于有机质的保存。

在海侵的影响下，泌阳凹陷核桃园组有机质富集的3个主要因素（初级生产力、保存条件和沉积速率）发生了变化。随着海侵程度的增加，有机质的初级生产力增加，沉积速率降低，这一过程导致有机质丰度增加和有机质质量提高，含油性增强，意味着海侵对湖相烃源岩的形成有积极影响[43]。

从页岩油可动性分布来看，潜江凹陷的页岩油可动性最好，其次是济阳坳陷、泌阳凹陷和辽河坳陷。潜江凹陷和济阳坳陷的OSI大部分数据点大于100 mg/g，而辽河坳陷的OSI数据点大多小于75 mg/g。从生烃潜力的分布可以看出，4个地区TOC与生烃潜力之间的相关性都很好，R^2（决定系数，取值0～1，值越大表示模型拟合越好）大于0.77，相邻拟合曲线之间的斜率差小于2，表明4个地区的生烃转化率相似。从含油性来看，潜江凹陷含油量最高，TOC和S_1+S_2含量较高，油气转化率最高，其次是泌阳凹陷、济阳坳陷，辽河坳陷含油性最差。

6　始新世咸化湖盆形成模式

典型咸化湖相页岩中有机质的富集受多种因素共同控制（图13），主要包括古氧化还原条件、陆源输入、古生产力、古盐度、古气候以及风化强度等。而对于油气富集而言，有机质的热演化转化效率和后期油气保存条件同样是决定性因素。

渤海湾盆地辽河坳陷位于较高纬度地区，在始新世时期受东亚夏季风影响较弱，风化程度较低，且未受到海

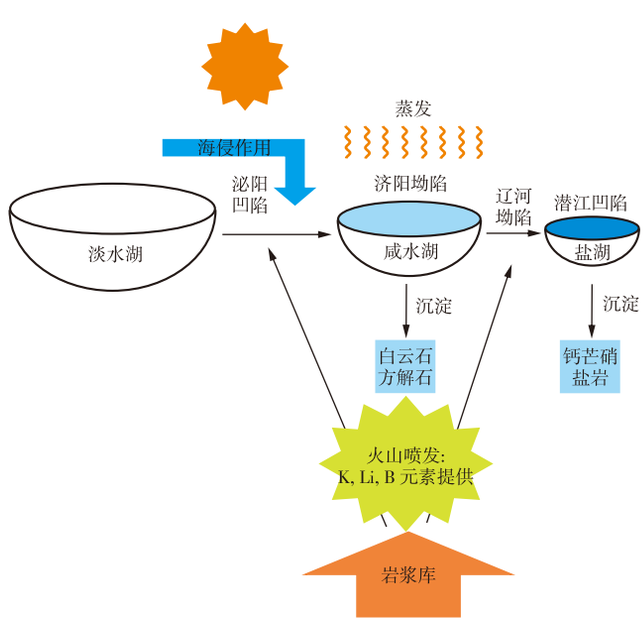

图13　中国东部盆地盐湖形成模式

Fig. 13　Formation model of salt lakes in basins of eastern China

侵作用。该地区火山活动频繁，对湖盆沉积环境产生显著影响。火山物质输入导致水体盐度偏低，有机质含量较低，但沉积过程中形成的还原环境有利于有机质热解转化，从而使生烃效率较高，页岩含油量相对较高（图14）。

渤海湾盆地济阳坳陷地处近海区域，在始新世时期受海侵作用显著。海水入侵使湖水矿化度升高，同时东亚夏季风作用增强，形成了中等风化强度的干热气候条件。沉积环境从弱氧化逐渐过渡到还原环境，为有机质的保存提供了良好条件。该区烃源岩有机质丰度高，页岩油含量大，且富含碳酸盐矿物，有利于形成优质储层并促进油气的生成与保存[136]（图14）。

南襄盆地泌阳凹陷在始新世时期也受到一定程度的海侵影响，但受东亚夏季风的影响相对较小。由于该区靠近内陆，风化程度低，湖水矿化度较低，气候以半湿润—干旱为主。沉积环境以弱氧化至氧化环境为主，不利于有机质的保存与转化，因而烃源岩TOC含量和含油量均较低（图14）。

江汉盆地潜江凹陷虽然位于内陆地区，但地处较低纬度，始新世时期受到强烈的东亚夏季风影响。该区气候干燥炎热，蒸发作用强烈，湖泊环境整体表现为高盐度特征。此外，潜江凹陷在始新世还受到频繁的火山活动与热液活动的双重影响。研究表明，火山灰降落与热液流体释放均能显著提升湖泊初级生产力[137-138]。火山及热液物质输入通过携带大量营养元素促进水体中浮游生物的繁殖，同时增加湖水盐度，强化水体分层，从而有利于有机质的沉积与保存[138]。此外，火山灰沉积所形成的水体分层阻隔了氧气的供给，减少了有机质的氧化作用，并在一定程度上防止了底层沉积物的扰动[139]。因此，潜江凹陷的页岩虽然整体TOC含量较低，但其生烃转化效率较高，表现出较强的生烃潜力（图14）。

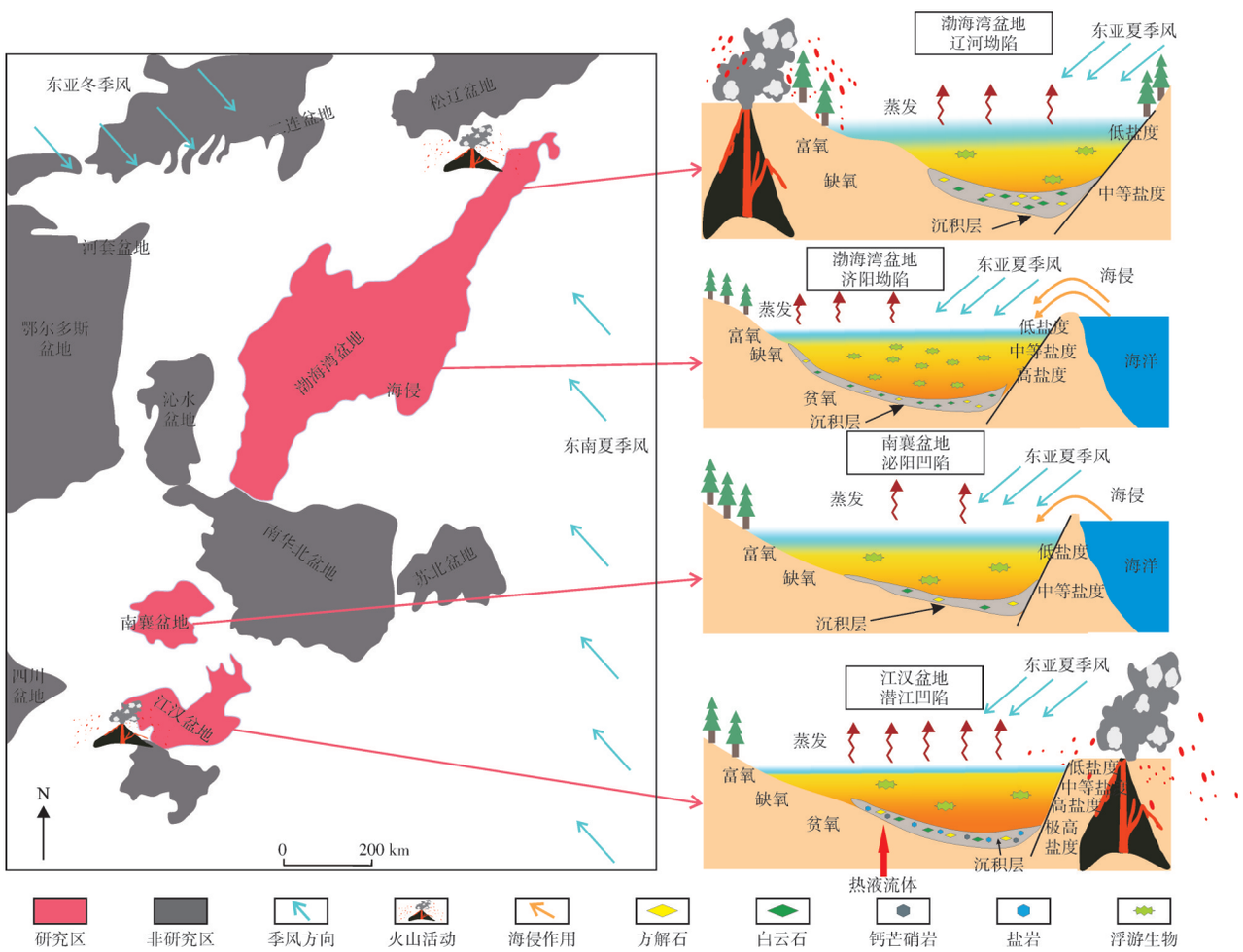

图14　中国东部盆地始新统页岩有机质富集模式

Fig. 14　Organic matter enrichment model of Eocene shale in basins of eastern China

7　结论

以中国东部辽河、济阳、泌阳及潜江等典型湖盆为例，对盐湖盆地始新统混合页岩的岩相特征及有机质富集机制进行系统研究，结合地球化学、沉积学与气候事件分析，对构造-气候-沉积耦合条件下的页岩岩相差异与有机质富集规律进行了综合探讨。主要结论如下：

1）全球气候变化、大气CO_2含量波动及东亚夏季风强度与各湖盆地球化学参数具有显著对应关系。在中始

新世暖期（约41～39 Ma），古气候、盐度及氧化还原条件均出现突变，反映湖泊体系对全球气候事件的敏感响应。

2）各研究区块有机物富集对气候响应一致，但区域间差异明显。辽河坳陷与潜江凹陷受火山活动影响显著，干热气候与火山灰沉积共同作用下有机质含量偏低，但火山灰覆盖有利于抑制有机质氧化与促进生烃转化。济阳坳陷与泌阳凹陷受海侵作用影响，海水输入提高湖盆水体盐度并携带营养物质，使页岩TOC含量较高。整体上，始新世湖盆表现出还原性由北向南增强的规律。

3）盐度变化对有机质的保存、生烃及油气运移具有关键控制作用。盐度与古气候-氧化还原条件的协同变化共同促进了富有机质页岩的形成。未来应加强古盐度重建及其与有机质分布的定量耦合研究，以深化对盐湖盆地页岩油成藏模式及控制机制的认识。

参 考 文 献

[1] Lazar O R, Bohacs K M, Schieber J, et al. Mudstone primer: lithofacies variations, diagnostic criteria, and sedimentologic-stratigraphic implications at lamina to bedset scale[M]. Tulsa, USA: SEPM Society for Sedimentary Geology, 2015.

[2] 邹才能, 董大忠, 王玉满, 等. 中国页岩气特征、挑战及前景(一)[J]. 石油勘探与开发, 2015, 42(6): 689-701.
Zou Caineng, Dong Dazhong, Wang Yuman, et al. Shale gas in China: Characteristics, challenges and prospects (Ⅰ)[J]. Petroleum Exploration and Development, 2015, 42(6): 689-701.

[3] Krumbein W C. The dispersion of fine-grained sediments for mechanical analysis[J]. Journal of Sedimentary Research, 1933, 3(3): 121-135.

[4] Picard M D. Classification of fine-grained sedimentary rocks[J]. Journal of Sedimentary Research, 1971, 41(1): 179-195.

[5] Land L S, Mack L E, Milliken K L, et al. Burial diagenesis of argillaceous sediment, south Texas Gulf of Mexico sedimentary basin: a reexamination[J]. Geological Society of America Bulletin, 1997, 109(1): 2-15.

[6] 刘惠民, 王勇, 李军亮, 等. 济阳坳陷始新统页岩岩相发育主控因素及分布特征[J]. 古地理学报, 2023, 25(4): 752-767.
Liu Huimin, Wang Yong, Li Junliang, et al. Main controlling factors and distribution characteristics of shale lithofacies in the Eocene of Jiyang Depression[J]. Journal of Palaeogeography (Chinese Edition), 2023, 25(4): 752-767.

[7] 宋光永, 刘占国, 王艳清, 等. 咸化湖盆混积岩岩相类型、沉积旋回及相模式: 以柴达木盆地风西地区新近系为例[J]. 石油勘探与开发, 2024, 51(6): 1304-1316.
Song Guangyong, Liu Zhanguo, Wang Yanqing, et al. Lithofacies types, sedimentary cycles, and facies models of saline lacustrine hybrid sedimentary rocks: a case study of Neogene in Fengxi area, Qaidam Basin, NW China[J]. Petroleum Exploration and Development, 2024, 51(6): 1304-1316.

[8] 谭先锋, 王萍, 王佳, 等. 早始新世极热气候时期咸化湖盆混合沉积作用: 以渤海湾盆地东营凹陷孔店组为例[J]. 石油与天然气地质, 2018, 39(2): 340-354.
Tan Xianfeng, Wang Ping, Wang Jia, et al. Mixed sedimentation in saline lacustrine basins during initial Eocene thermal maximum period: a case study on Kongdian Formation in Dongying Sag, Bohai Bay Basin[J]. Oil & Gas Geology, 2018, 39(2): 340-354.

[9] 尹嘉, 邹才能, 吴松涛, 等. 咸化湖盆优质烃源岩发育机制与页岩油富集过程: 以柴达木盆地下干柴沟组上段为例[J]. 地球科学, 2025, 50(7): 2875-2898.
Yin Jia, Zou Caineng, Wu Songtao, et al. Development mechanism of high-quality source rock and enrichment processes of shale oil in saline lacustrine basin: a case study of Upper member of Lower Ganchaigou Formation, Qaidam Basin[J]. Earth Science, 2025, 50(7): 2875-2898.

[10] 荆铁亚, 王金意, 毛俊莉, 等. 断陷湖盆页岩油形成的地质要素匹配: 以辽河西部凹陷沙三段为例[J]. 地质科技情报, 2016, 35(5): 148-153.
Jing Tieya, Wang Jinyi, Mao Junli, et al. Geological factors matching of shale oil accumulation in rifted lacustrine basins: a case study from 3rd member of Shahejie formation in Liaohe western depression [J]. Geological Science and Technology Information, 2016, 35(5): 148-153.

[11] 苏宗富, 邓宏文, 陶宗普, 等. 济阳坳陷古近系区域层序地层格架地层特征对比[J]. 古地理学报, 2006, 8(1): 89-102.
Su Zongfu, Deng Hongwen, Tao Zongpu, et al. Correlation of stratigraphic features in regional sequence stratigraphic framework of the Paleogene in Jiyang Depression[J]. Journal of Palaeogeography, 2006, 8(1): 89-102.

[12] 张文伟. 基于主(微)量元素分析法的细粒沉积岩沉积环境判别: 以大民屯凹陷安福屯地区沈352井沙四下亚段为例[J]. 东北石油大学学报, 2017, 41(4): 99-106.
Zhang Wenwei. Identification of sedimentary environment of fine-grained sedimentary rock based on major(trace)elements analysis: taking the lower fourth member of Shahejie formation in the well of Shen 352 of Anfutun area of Damintun depression for example[J]. Journal of Northeast Petroleum University, 2017, 41(4): 99-106.

[13] 王必金. 江汉盆地构造演化与勘探方向[D]. 北京: 中国地质大学(北京), 2006.
Wang Bijin. The structural evolution and favorable exploration areas in Jianghan basin[D]. Beijing: China University of Geosciences, 2006.

[14] 单衍胜. 辽河坳陷古近系页岩油气聚集条件与分布[D]. 北京: 中国地质大学(北京), 2013.
Dan Yansheng. Accumulation conditions and distribution of shale oil and gas in the Paleogene of the Liaohe Depression[D]. Beijing: China University of Geosciences (Beijing), 2013.

[15] 孔凡飞. 济阳坳陷牛页1井古近系陆相细粒岩沉积机制[D]. 青岛: 山东科技大学, 2019.
Kong Fanfei. Sedimentary mechanism of Paleogene continental fine grained rocks in Niuye 1 Well, Jiyang Depression[D]. Qingdao: Shandong University of Science and Technology, 2019.

[16] 李辉. 泌阳凹陷古城—高庄复杂断裂带构造特征及控油作用[D]. 北京: 中国地质大学(北京), 2009.
Li Hui. Structural characteristics and oil controlling effect of the complex fault zone between Gucheng and Gaozhuang in the Biyang Depression[D]. Beijing: China University of Geosciences Beijing, 2009.

[17] 苏奥. 中国东部南襄盆地泌阳凹陷核桃园组湖相页岩的有机质富集及古气候记录[D]. 武汉: 中国地质大学(武汉), 2020.

Su Ao. Organic matter enrichment and paleoclimatic records of lacustrine shale in the Walnut Garden Formation of the Biyang Depression, Nanxiang Basin, eastern China[D]. Wuhan: China University of Geosciences (Wuhan), 2020.

[18] Teng X, Fang X, Kaufman A J, et al. Sedimentological and mineralogical records from drill core SKD1 in the Jianghan Basin, Central China, and their implications for Late Cretaceous–early Eocene climate change[J]. Journal of Asian Earth Sciences, 2019, 182: 103936.

[19] Shen C B, Donelick R A, O'Sullivan P B, et al. Provenance and hinterland exhumation from LA-ICP-MS zircon U-Pb and fission-track double dating of Cretaceous sediments in the Jianghan Basin, Yangtze block, Central China[J]. Sedimentary Geology, 2012, 281: 194–207.

[20] Wu L, Mei L, Liu Y, et al. Multiple provenance of rift sediments in the composite basin-mountain system: constraints from detrital zircon U-Pb geochronology and heavy minerals of the early Eocene Jianghan Basin, Central China[J]. Sedimentary Geology, 2017, 349: 46–61.

[21] Yu X, Wang C, Liu C, et al. Sedimentary characteristics and depositional model of a Paleocene–Eocene salt lake in the Jiangling depression, China[J]. Chinese Journal of Oceanology and Limnology, 2015, 33(6): 1426–1435.

[22] Yan K, Wang C, Liu C, et al. Reconstruction of early Paleogene landscapes and climate in the Jianghan Basin, Central China: evidence from evaporites and palynology[J]. Palaeogeography, Palaeoclimatology, Palaeoecology, 2022, 601: 111095.

[23] 蔡惠慧. 始新世全球变冷过程中的温室气候模拟研究[D]. 成都: 成都理工大学, 2014.
Cai Huihui. Simulation study on greenhouse climate during the global cooling process in the Eocene epoch[D]. Chengdu: Chengdu University of Technology, 2014.

[24] Sun D, Liu D, Chen M, et al. Magnetostratigraphy and palaeoclimate of red clay sequences from Chinese Loess Plateau[J]. Science in China Series D: Earth Sciences, 1997, 40(4): 337–343.

[25] 王大宁, 孙秀玉, 赵英娘. 河南西部潭头盆地古新世—始新世孢粉植物群[J]. 植物学报, 1984, 26(4): 448–455.
Wang Daning, Sun Xiuyu, Zhao Yingniang. The Paleocene–Eocene Palynoflora from the Tantou Basin in West Henan[J]. Journal of Integrative Plant Biology, 1984, 26(4): 448–455.

[26] Sun X, Wang P. How old is the Asian monsoon system? : palaeobotanical records from China[J]. Palaeogeography, Palaeoclimatology, Palaeoecology, 2005, 222(3): 181–222.

[27] Kennett J P, Stott L D. Abrupt deep-sea warming, palaeoceanographic changes and benthic extinctions at the end of the Palaeocene[J]. Nature, 1991, 353(6341): 225–229.

[28] Zachos J, Pagani M, Sloan L, et al. Trends, rhythms, and aberrations in global climate 65 MA to present[J]. Science, 2001, 292(5517): 686–693.

[29] Zachos J C, Dickens G R, Zeebe R E. An early Cenozoic perspective on greenhouse warming and carbon-cycle dynamics[J]. Nature, 2008, 451(7176): 279–283.

[30] Zeebe R E, Zachos J C. Long-term legacy of massive carbon input to the Earth system: Anthropocene versus Eocene[J]. Philosophical Transactions of the Royal Society A: Mathematical, Physical and Engineering Sciences, 2013, 371(2001): 20120006.

[31] Li M, Bralower T J, Kump L R, et al. Astrochronology of the Paleocene–Eocene thermal maximum on the Atlantic coastal plain[J]. Nature Communications, 2022, 13: 5618.

[32] Li Y, Sun P, Zhang Q, et al. Middle Eocene Climatic Optimum sensitivity of a continental lake basin from geochemical records of the Fushun Basin, Northeastern China[J]. Ore Geology Reviews, 2023, 161: 105637.

[33] Xiao G, Zhang Z, Yao Z. The Eocene–Oligocene climate transition: review of recent progress[J]. Geological Review, 2012, 58(1): 91–105.

[34] Sluijs A, Zeebe R E, Bijl P K, et al. A middle Eocene carbon cycle conundrum[J]. Nature Geoscience, 2013, 6(6): 429–434.

[35] Röhl U, Westerhold T, Bralower T J, et al. On the duration of the Paleocene–Eocene thermal maximum (PETM) [J]. Geochemistry, Geophysics, Geosystems, 2007, 8(12): 2007GC001784.

[36] 李元吉. 抚顺盆地古近纪古环境演化与有机质富集机制研究[D]. 长春: 吉林大学, 2022.
Li Yuanji. Paleogene Paleoenvironmental evolution and organic matter accumulation mechanisms, Fushun Basin[D]. Changchun: Jilin University, 2022.

[37] 葛瑞全, 宋传春, 淳萍, 等. 济阳沾-车凹陷古近系沙河街组海侵的再认识[J]. 高校地质学报, 2003, 9(3): 450–457.
Ge Ruiquan, Song Chuanchun, Chun Ping, et al. Restudy on the Shahejie formation transgression of the Paleogene in Zhan-Che Sag (Jiyang depression) [J]. Geological Journal of China Universities, 2003, 9(3): 450–457.

[38] 王冠民, 钟建华, 姜在兴, 等. 从济阳坳陷沙一段古盐度的横向变化看古近纪的海侵方向[J]. 世界地质, 2005, 24(3): 243–247.
Wang Guanmin, Zhong Jianhua, Jiang Zaixing, et al. Possible transgressive channel in Paleogene deduced by lateral change of palaeosalinity in 1st Member of Shahejie Formation in Jiyang depression[J]. World Geology, 2005, 24(3): 243–247.

[39] 袁文芳, 陈世悦, 曾昌民. 渤海湾盆地古近纪海侵问题研究进展及展望[J]. 沉积学报, 2005, 23(4): 604–612.
Yuan Wenfang, Chen Shiyue, Zeng Changmin. Research development and prospects on Paleogene Sea transgression in Bohai Bay Basin[J]. Acta Sedimentologica Sinica, 2005, 23(4): 604–612.

[40] 袁文芳, 陈世悦, 曾昌民. 济阳坳陷古近系沙河街组海侵问题研究[J]. 石油学报, 2006, 27(4): 40–44.
Yuan Wenfang, Chen Shiyue, Zeng Changmin. Study on marine transgression of Paleogene shahejie formation in Jiyang depression [J]. Acta Petrolei Sinica, 2006, 27(4): 40–44.

[41] 袁文芳, 曾昌民, 陈世悦. 济阳坳陷古近纪咸化层段甲藻甾烷和C_{31}甾烷特征[J]. 沉积学报, 2008, 26(4): 683–687.
Yuan W, Zeng C, Chen S. Characteristic of dinosterane and C_{31} sterane in Paleocene saline formation of Jiyang depression[J]. Acta Sedimentologica Sinica, 2008, 26(4): 683–687.

[42] Chen Z, Huang W, Liu Q, et al. Geochemical characteristics of the Paleogene shales in the Dongying depression, Eastern China[J]. Marine and Petroleum Geology, 2016, 73: 249–270.

[43] Xia L, Cao J, Hu S, et al. How marine incursion influences the quality of lacustrine source rocks: the Paleogene Nanxiang Basin, Eastern China[J]. AAPG Bulletin, 2019, 103(5): 1071–1096.

[44] Hou D, Li M, Huang Q. Marine transgressional events in the gigantic freshwater lake Songliao: paleontological and geochemical evidence

[J]. Organic Geochemistry, 2000, 31(7/8): 763-768.

[45] Li Maowen, Pang Xiongqi. Contentious petroleum geochemical issues in China's sedimentary basins[J]. Petroleum Science, 2004, 1(3): 4-22.

[46] Ding W, Wan H, Zhang Y, et al. Characteristics of the Middle Jurassic marine source rocks and prediction of favorable source rock kitchens in the Qiangtang Basin of Tibet[J]. Journal of Asian Earth Sciences, 2013, 66: 63-72.

[47] Erbacher J, Huber B T, Norris R D, et al. Increased thermohaline stratification as a possible cause for an ocean anoxic event in the Cretaceous period[J]. Nature, 2001, 409(6818): 325-327.

[48] Wei W, Algeo T J, Lu Y, et al. Identifying marine incursions into the Paleogene Bohai Bay Basin lake system in northeastern China[J]. International Journal of Coal Geology, 2018, 200: 1-17.

[49] Jagniecki E A, Lowenstein T K. Evaporites of the Green river formation, Bridger and Piceance Creek basins: deposition, diagenesis, paleobrine chemistry, and Eocene atmospheric CO_2[M]// Stratigraphy and paleolimnology of the green river formation, western USA. Dordrecht: Springer Netherlands, 2015: 277-312.

[50] Lowenstein T K, Jagniecki E A, Carroll A R, et al. The Green River salt mystery: what was the source of the hyperalkaline lake waters? [J]. Earth-Science Reviews, 2017, 173: 295-306.

[51] 李毅, 方石, 孙平昌, 等. 辽河盆地西部凹陷沙河街组古近系页岩气成藏地质条件研究[J]. 地质与资源, 2017, 26(2): 140-146.
Li Yi, Fang Shi, Sun Pingchang, et al. Geological conditions of shale gas accumulation of Paleogene Shahejie formation in the western sag of Liaohe basin[J]. Geology and Resources, 2017, 26(2): 140-146.

[52] He J, Cai J, Lei T, et al. Characteristics comparison and occurrence mode of different types of soluble organic matter in lacustrine shale in the Dongying Sag, Eastern China[J]. International Journal of Coal Geology, 2022, 254: 103971.

[53] 陶光辉, 丁连民, 赵林, 等. 泌阳凹陷页岩储层物理化学性质对井壁稳定性影响的实验研究[J]. 科学技术与工程, 2020, 20(15): 6018-6025.
Tao Guanghui, Ding Lianmin, Zhao Lin, et al. Experimental study on influence of physicochemical properties of shale reservoir in Biyang depression on borehole stability[J]. Science Technology and Engineering, 2020, 20(15): 6018-6025.

[54] Sun Z, He Z, Wang F, et al. Occurrence characteristics of saline-lacustrine shale-oil in the Qianjiang depression, Jianghan Basin, Central China[J]. Journal of Earth Science, 2022, 33(4): 945-962.

[55] 吕艳南. 辽河西部凹陷沙三、沙四段页岩油形成条件及发育模式[D]. 北京: 中国地质大学(北京), 2016.
Lyu Yannan. Formation conditions and development patterns of shale oil in the Sha-3 and Sha-4 sections of the western depression of Liaohe River[D]. Beijing: China University of Geosciences Beijing, 2016.

[56] Wang A, Wang Z, Liu J, et al. The Sr/Ba ratio response to salinity in clastic sediments of the Yangtze River Delta[J]. Chemical Geology, 2021, 559: 119923.

[57] Li P, Liu Z B, Bi H, et al. Differences in and factors controlling organic matter enrichment in the Ziliujing Formation shale in the Sichuan Basin[J]. Petroleum Science, 2024, 21(1): 77-86.

[58] 周靖皓, 鲜本忠, 张建国, 等. 高频旋回地层约束下的湖相页岩有机质富集规律: 以东营凹陷古近系沙三下亚段为例[J]. 古地理学报, 2022, 24(4): 759-770.
Zhou Jinghao, Xian Benzhong, Zhang Jianguo, et al. Organic matter enrichment law of lacustrine shale constrained by high resolution cyclostratigraphy: a case study from the Lower sub-member of Member 3 of Paleogene Shahejie Formation, Dongying sag[J]. Journal of Palaeogeography (Chinese Edition), 2022, 24(4): 759-770.

[59] 田德瑞, 牛成民, 王德英, 等. 渤海海域辽西凹陷中央反转带原油成因类型及成藏特征[J]. 高校地质学报, 2021, 27(4): 444-458.
Tian Derui, Niu Chengmin, Wang Deying, et al. Genetic types and accumulation of crude oil in the central inversion zone in the Liaoxi depression, Bohai Sea[J]. Geological Journal of China Universities, 2021, 27(4): 444-458.

[60] 陈晨, 姜在兴, 孔祥鑫, 等. 潜江凹陷潜江组盐间细粒岩沉积特征及其对页岩含油性的控制[J]. 地学前缘, 2021, 28(5): 421-435.
Chen Chen, Jiang Zaixing, Kong Xiangxin, et al. Sedimentary characteristics of intersalt fine-grained sedimentary rocks and their control on oil-bearing ability of shales in the Qianjiang Formation, Qianjiang Sag[J]. Earth Science Frontiers, 2021, 28(5): 421-435.

[61] 郭来源. 陆相断陷湖盆富有机质页岩非均质性及其控制因素分析[D]. 武汉: 中国地质大学, 2017.
Guo Laiyuan. Heterogeneity and controlling factors of organic-rich shale in continental rift basin[D]. Wuhan: China University of Geosciences, 2017.

[62] Mcarthur J M, Algeo T J, Van De Schootbrugge B, et al. Basinal restriction, black shales, re-Os dating, and the Early Toarcian (Jurassic) oceanic anoxic event[J]. Paleoceanography, 2008, 23(4): 2008PA001607.

[63] Nesbitt H W, Young G M. Early Proterozoic climates and plate motions inferred from major element chemistry of lutites[J]. Nature, 1982, 299(5885): 715-717.

[64] Visser J N J, Young G M. Major element geochemistry and paleoclimatology of the Permo-Carboniferous glacigene Dwyka Formation and postglacial mudrocks in southern Africa[J]. Palaeogeography, Palaeoclimatology, Palaeoecology, 1990, 81(1-2): 49-57.

[65] Young G M. Geochemical investigation of a Neoproterozoic glacial unit: the Mineral Fork formation in the Wasatch Range, Utah[J]. Geological Society of America Bulletin, 2002, 114(4): 387-399.

[66] Von Allmen K, Böttcher M E, Samankassou E, et al. Barium isotope fractionation in the global barium cycle: first evidence from barium minerals and precipitation experiments[J]. Chemical Geology, 2010, 277(1-2): 70-77.

[67] Paiste K, Pellerin A, Zerkle A L, et al. The pyrite multiple sulfur isotope record of the 1.98 Ga Zaonega Formation: evidence for biogeochemical sulfur cycling in a semi-restricted basin[J]. Earth and Planetary Science Letters, 2020, 534: 116092.

[68] Sullivan M D, Haszeldine R S, Fallick A E. Linear coupling of carbon and strontium isotopes in Rotliegend Sandstone, North Sea: evidence for cross-formational fluid flow[J]. Geology, 1990, 18(12): 1215-1218.

[69] Van Os B J H, Middelburg J J, De Lange G J. Possible diagenetic mobilization of barium in sapropelic sediment from the eastern Mediterranean[J]. Marine Geology, 1991, 100(1-4): 125-136.

[70] Kabata-Pendias A. Trace elements in soils and plants[M]. Boca Raton: CRC Press, 2010.

[71] Dymond J, Suess E, Lyle M. Barium in deep-sea sediment: a geochemical proxy for paleoproductivity[J]. Paleoceanography, 1992, 7(2): 163-181.

[72] Algeo T J, Maynard J B. Trace-element behavior and redox facies in core shales of Upper Pennsylvanian Kansas-type cyclothems[J]. Chemical Geology, 2004, 206(3-4): 289-318.

[73] Tribovillard N, Algeo T J, Lyons T, et al. Trace metals as paleoredox and paleoproductivity proxies: an update[J]. Chemical Geology, 2006, 232(1-2): 12-32.

[74] 李明龙, 郑德顺, 戴光忠, 等. 豫西济源盆地侏罗系泥质岩地球化学特征及其环境和物源示踪[J]. 地质学报, 2014, 88(2): 228-238.
Li Minglong, Zheng Deshun, Dai Guangzhong, et al. Geochemical characteristics of the Jurassic argillaceous rocks of the Jiyuan Basin, Western Henan and the implications for environments and provenances[J]. Acta Geologica Sinica, 2014, 88(2): 228-238.

[75] Murphy A E, Sageman B B, Hollander D J, et al. Black shale deposition and faunal overturn in the Devonian Appalachian Basin: clastic starvation, seasonal water-column mixing, and efficient biolimiting nutrient recycling[J]. Paleoceanography, 2000, 15(3): 280-291.

[76] Campos Alvarez N O, Roser B P. Geochemistry of black shales from the Lower Cretaceous Paja Formation, Eastern Cordillera, Colombia: source weathering, provenance, and tectonic setting[J]. Journal of South American Earth Sciences, 2007, 23(4): 271-289.

[77] Sinha S, Islam R, Ghosh S K, et al. Geochemistry of Neogene Siwalik mudstones along Punjab re-entrant, India: implications for source-area weathering, provenance and tectonic setting[J]. Current Science, 2023, 92(8): 1103-1113.

[78] Kasanzu C, Maboko M A H, Manya S. Geochemistry of fine-grained clastic sedimentary rocks of the Neoproterozoic Ikorongo Group, NE Tanzania: implications for provenance and source rock weathering[J]. Precambrian Research, 2008, 164(3-4): 201-213.

[79] Zaghloul M N, Critelli S, Perri F, et al. Depositional systems, composition and geochemistry of Triassic rifted-continental margin redbeds of the Internal Rif Chain, Morocco[J]. Sedimentology, 2010, 57(2): 312-350.

[80] Von Eynatten H. Petrography and chemistry of sandstones from the Swiss Molasse Basin: an archive of the Oligocene to Miocene evolution of the Central Alps[J]. Sedimentology, 2003, 50(4): 703-724.

[81] Montero-Serrano J C, Föllmi K B, Adatte T, et al. Continental weathering and redox conditions during the early Toarcian Oceanic Anoxic Event in the northwestern Tethys: insight from the Posidonia Shale section in the Swiss Jura Mountains[J]. Palaeogeography, Palaeoclimatology, Palaeoecology, 2015, 429: 83-99.

[82] Ma Y, Fan M, Lu Y, et al. Climate-driven paleolimnological change controls lacustrine mudstone depositional process and organic matter accumulation: constraints from lithofacies and geochemical studies in the Zhanhua Depression, Eastern China[J]. International Journal of Coal Geology, 2016, 167: 103-118.

[83] Liang C, Wu J, Jiang Z, et al. Sedimentary environmental controls on petrology and organic matter accumulation in the Upper fourth member of the Shahejie Formation (Paleogene, Dongying depression, Bohai Bay Basin, China)[J]. International Journal of Coal Geology, 2018, 186: 1-13.

[84] Li W, Lu S, Tan Z, et al. Lacustrine source rock deposition in response to coevolution of the paleoenvironment and formation mechanism of organic-rich shales in the Biyang depression, Nanxiang Basin[J]. Energy & Fuels, 2017, 31(12): 13519-13527.

[85] 徐崇凯. 江汉盆地潜江凹陷咸化特征与烃源岩发育的关系[D]. 西安: 西北大学, 2018.
Xu Chongkai. The relationship between salty characteristics and source rock formation in Qianjiang sag, Jianghan basin[D]. Xi'an: Northwest University, 2018.

[86] 张妮, 武毅, 张霞, 等. 辽河坳陷大民屯凹陷古近系沙河街组三段地球化学特征及其地质意义[J]. 地质学报, 2021, 95(2): 517-535.
Zhang Ni, Wu Yi, Zhang Xia, et al. Geochemical characteristics and its implications of the third Member of Paleogene Shahejie Formation from the Damintun sag, Liaohe depression[J]. Acta Geologica Sinica, 2021, 95(2): 517-535.

[87] Wu J, Liang C, Yang R, et al. Sequence stratigraphic control on the variations of organic matter in Eocene lacustrine shales within the Dongying Depression, Eastern China[J]. Journal of Asian Earth Sciences, 2022, 237: 105353.

[88] Tan Z, Lu S, Li W, et al. Climate-driven variations in the depositional environment and organic matter accumulation of lacustrine mudstones: evidence from organic and inorganic geochemistry in the Biyang depression, Nanxiang Basin, China[J]. Energy & Fuels, 2019, 33(8): 6946-6960.

[89] Ge T, Jiang Z, Kong X, et al. Salt rhythmite formation and organic matter enrichment in the Qianjiang formation, Jianghan Basin, China: constraints from alternating dry and wet climates[J]. Marine and Petroleum Geology, 2023, 148: 106067.

[90] Wang Z, Liu G, Gao P, et al. Geochemistry of source rocks and oil-source rock correlation in the Hetaoyuan Formation of the Nanyang Sag, Nanxiang Basin, Eastern China[J]. Geological Journal, 2018, 53 (5): 2334-2351.

[91] 尚飞, 刘峥君, 解习农, 等. 泌阳凹陷核三段主力富有机质页岩层地球化学特征[J]. 新疆石油地质, 2015, 36(1): 42-47.
Shang Fei, Liu Zhengjun, Xie Xinong, et al. Geochemical characteristics of organic-rich shales of He-3 member of Hetaoyuan formationin Biyang Sag[J]. Xinjiang Petroleum Geology, 2015, 36(1): 42-47.

[92] 侯庆杰, 金强, 牛成民, 等. 辽东湾地区主力烃源岩分布特征与主控因素[J]. 地球科学, 2018, 43(6): 2160-2171.
Hou Qingjie, Jin Qiang, Niu Chengmin, et al. Distribution characteristics and main controlling factors of main hydrocarbon source rocks in Liaodong Bay area[J]. Earth Science, 2018, 43(6): 2160-2171.

[93] Liang C, Wu J, Cao Y, et al. Storage space development and hydrocarbon occurrence model controlled by lithofacies in the Eocene Jiyang Sub-basin, East China: significance for shale oil reservoir formation[J]. Journal of Petroleum Science and Engineering, 2022, 215: 110631.

[94] Stuiver M. Climate versus changes in ^{13}C content of the organic component of lake sediments during the Late Quaternary[J]. Quaternary Research, 1975, 5(2): 251-262.

[95] Horton T W, Defliese W F, Tripati A K, et al. Evaporation induced ^{18}O and ^{13}C enrichment in lake systems: a global perspective on hydrologic balance effects[J]. Quaternary Science Reviews, 2016,

131: 365-379.

[96] Mckenzie D. The extraction of magma from the crust and mantle[J]. Earth and Planetary Science Letters, 1985, 74(1): 81-91.

[97] Talbot M R. A review of the palaeohydrological interpretation of carbon and oxygen isotopic ratios in primary lacustrine carbonates[J]. Chemical Geology: Isotope Geoscience Section, 1990, 80(4): 261-279.

[98] 李得立, 谭先锋, 夏敏全, 等. 东营凹陷沙四段湖相白云岩沉积特征及成因[J]. 断块油气田, 2010, 17(4): 418-422.
Li Deli, Tan Xianfeng, Xia Minquan, et al. Sedimentary characteristics and genesis of lacustrine dolomite in the fourth member of Shahejie Formation in Dongying Sag[J]. Fault-Block Oil & Gas Field, 2010, 17(4): 418-422.

[99] 滕建彬. 东营凹陷利页1井泥页岩中白云石成因及层序界面意义[J]. 油气地质与采收率, 2018, 25(2): 1-7.
Teng Jianbin. Genesis of dolomite in shale drilled by Well Liye1 in Dongying Sag and its significance on sequence boundary indication [J]. Petroleum Geology and Recovery Efficiency, 2018, 25(2): 1-7.

[100] 滕建彬, 邱隆伟, 张守鹏, 等. 济阳坳陷古近系沙河街组湖相富有机质页岩白云石成因及成岩演化[J]. 石油勘探与开发, 2022, 49(6): 1080-1093.
Teng Jianbin, Qiu Longwei, Zhang Shoupeng, et al. Origin and diagenetic evolution of dolomites in paleogene Shahejie Formation lacustrine organic shale of jiyang depression, bohai bay basin, east China[J]. Petroleum Exploration and Development, 2022, 49(6): 1080-1093.

[101] 刘万洙, 王璞珺. 松辽盆地嫩江组白云岩结核的成因及其环境意义[J]. 岩相古地理, 1997, 17(1): 22-26.
Liu Wanzhu, Wang Pujun. Genesis and environmental significance of the dolomite concretions from the Nenjiang formation in the Songliao basin, northeast ern China[J]. Sedimentary Facies and Palaeogeography, 1997, 17(1): 22-26.

[102] 王国栋, 程日辉, 王璞珺, 等. 松辽盆地嫩江组白云岩形成机理: 以松科1井南孔为例[J]. 地质学报, 2008, 82(1): 48-54.
Wang Guodong, Cheng Rihui, Wang Pujun, et al. The forming mechanism of dolostone of Nenjiang Formation in Songliao Basin: example from CCSD-SK II[J]. Acta Geologica Sinica, 2008, 82(1): 48-54.

[103] 付秀丽, 蒙启安, 文政, 等. 松辽盆地白云岩沉积环境及成因机理[J]. 沉积学报, 2024, 42(1): 113-129.
Fu Xiuli, Meng Qi'an, Wen Zheng, et al. Sedimentary environment and genetic mechanism of dolomites in the Qingshankou formation, Songliao Basin[J]. Acta Sedimentologica Sinica, 2024, 42(1): 113-129.

[104] Yang J H, Yi C L, Du Y S, et al. Geochemical significance of the Paleogene soda-deposits bearing strata in Biyang Depression, Henan Province[J]. Science China Earth Sciences, 2015, 58(1): 129-137.

[105] 李红, 柳益群, 梁浩, 等. 新疆三塘湖盆地中二叠统芦草沟组湖相白云岩成因[J]. 古地理学报, 2012, 14(1): 45-58.
Li Hong, Liu Yiqun, Liang Hao, et al. Origin of lacustrine dolostones of the Middle Permian Lucaogou formation in santanghu basin of Xinjiang[J]. Journal of Palaeogeography, 2012, 14(1): 45-58.

[106] Wen H, Zheng R, Qing H, et al. Primary dolostone related to the Cretaceous lacustrine hydrothermal sedimentation in Qingxi sag, Jiuquan Basin on the northern Tibetan Plateau[J]. Science China Earth Sciences, 2013, 56(12): 2080-2093.

[107] 王兵杰, 蔡明俊, 林春明, 等. 渤海湾盆地塘沽地区古近系沙河街组湖相白云岩特征及成因[J]. 古地理学报, 2014, 16(1): 65-76.
Wang Bingjie, Cai Mingjun, Lin Chunming, et al. Characteristics and origin of lacustrine dolostone of the Paleogene Shahejie Formation in Tanggu area, Bohai Bay Basin[J]. Journal of Palaeogeography, 2014, 16(1): 65-76.

[108] 宋柏荣, 韩洪斗, 崔向东, 等. 渤海湾盆地辽河坳陷古近系沙河街组四段湖相方沸石白云岩成因分析[J]. 古地理学报, 2015, 17(1): 33-44.
Song Bairong, Han Hongdou, Cui Xiangdong, et al. Petrogenesis analysis of lacustrine analcite dolostone of the Member 4 of Paleogene Shahejie Formation in Liaohe Depression, Bohai Bay Basin [J]. Journal of Palaeogeography, 2015, 17(1): 33-44.

[109] 曲长胜, 邱隆伟, 杨勇强, 等. 吉木萨尔凹陷芦草沟组碳酸盐岩碳氧同位素特征及其古湖泊学意义[J]. 地质学报, 2017, 91(3): 605-616.
Qu Changsheng, Qiu Longwei, Yang Yongqiang, et al. Carbon and oxygen isotope compositions of carbonatic rock from Permian Lucaogou Formation in the Jimsar Sag, NW China and their paleolimnological significance[J]. Acta Geologica Sinica, 2017, 91 (3): 605-616.

[110] 魏巍, 朱筱敏, 朱世发, 等. 二连盆地阿南凹陷下白垩统腾格尔组湖相云质岩成因[J]. 地球科学, 2017, 42(2): 258-272.
Wei Wei, Zhu Xiaomin, Zhu Shifa, et al. Origin of lacustrine dolomitic rocks of the Lower Cretaceous tengge'er formation in anan sag, erlian basin[J]. Earth Science, 2017, 42(2): 258-272.

[111] Zhang S, Liu Y Q, Li H, et al. Hydrothermal-sedimentary dolomite: a case from the Middle Permian in eastern Junggar Basin, China[J]. Journal of Palaeogeography, 2020, 9(4): 415-437.

[112] Yang Z, Zhong D, Whitaker F, et al. Syn-sedimentary hydrothermal Dolomites in a lacustrine rift basin: petrographic and geochemical evidence from the Lower Cretaceous Erlian Basin, Northern China[J]. Sedimentology, 2020, 67(1): 305-329.

[113] Wu A, Cao J, Zhang J, et al. Origin of microbial-hydrothermal bedded Dolomites in the Permian Lucaogou Formation lacustrine shales, Junggar Basin, NW China[J]. Sedimentary Geology, 2022, 440: 106260.

[114] Liu X, Tarantola A, Chen H, et al. Middle Eocene Paleoclimate recorded in halite deposits in Jianghan Basin, Central China[J]. Marine and Petroleum Geology, 2023, 153: 106305.

[115] He J, Ding W, Jiang Z, et al. Mineralogical and chemical distribution of the Es^3 L oil shale in the Jiyang Depression, Bohai Bay Basin (E China): implications for paleoenvironmental reconstruction and organic matter accumulation[J]. Marine and Petroleum Geology, 2017, 81: 196-219.

[116] Wang Q, Hao F, Xu C, et al. Paleolimnological environments and the formation of high quality source rocks in the Bohai Bay Basin: an integrated geochemical study of biomarkers, stable carbon and oxygen isotopes, and trace elements[J]. Journal of Petroleum Science and Engineering, 2020, 195: 107753.

[117] 朱芳冰, 周红. 辽河盆地西部凹陷沙河街组砂岩碳酸盐胶结物特征[J]. 地球科学, 2022, 47(12): 4724-4730.
Zhu Fangbing, Zhou Hong. Characteristics of carbonate cements in sandstone of shahejie formation in western depression, Liaohe Basin [J]. Earth Science, 2022, 47(12): 4724-4730.

[118] Su A, Bons P D, Chen H, et al. Age, material source, and formation mechanism of bedding-parallel calcite beef veins: case from the mature Eocene lacustrine shales in the Biyang Sag, Nanxiang Basin, China[J]. Geological Society of America Bulletin, 2022, 134(7-8): 1811-1833.

[119] Zhu S, Qin Y, Liu X, et al. Origin of dolomitic rocks in the Lower Permian Fengcheng formation, Junggar Basin, China: evidence from petrology and geochemistry[J]. Mineralogy and Petrology, 2017, 111(2): 267-282.

[120] Guo P, Wen H, Gibert L, et al. Deposition and diagenesis of the Early Permian volcanic-related alkaline playa-lake dolomitic shales, NW Junggar Basin, NW China[J]. Marine and Petroleum Geology, 2021, 123: 104780.

[121] Yu K, Zhang Z, Cao Y, et al. Origin of biogenic-induced cherts from Permian alkaline saline lake deposits in the NW Junggar Basin, NW China: implications for hydrocarbon exploration[J]. Journal of Asian Earth Sciences, 2021, 211: 104712.

[122] 王俊怀, 刘英辉, 万策, 等. 准噶尔盆地乌—夏地区二叠系风城组云质岩特征及成因[J]. 古地理学报, 2014, 16(2): 157-168.
Wang Junhuai, Liu Yinghui, Wan Ce, et al. Characteristics and origin of dolomitic tuff in the Permian Fengcheng Formation in Wu-Xia area of Junggar Basin[J]. Journal of Palaeogeography, 2014, 16(2): 157-168.

[123] Wang T, Cao J, Xia L, et al. Revised age of the Fengcheng Formation, Junggar Basin, China: global implications for the Late Paleozoic ice age[J]. Global and Planetary Change, 2022, 208: 103725.

[124] 刘英辉. 准噶尔盆地乌—夏地区风城组云质岩类沉积环境及成因探讨[J]. 吉林大学学报(地球科学版), 2022, 52(1): 80-93.
Liu Yinghui. Origin of dolomitic tuff in Permian Fengcheng Formation in Wu-Xia area of Junggar Basin[J]. Journal of Jilin University (Earth Science Edition), 2022, 52(1): 80-93.

[125] 蔡媛, 孔祥鑫, 姜在兴, 等. 潜江凹陷古近系盐间地层沉积环境与有机质富集: 以潜江组三段下亚段10号韵律为例[J]. 石油学报, 2022, 43(5): 605-616.
Cai Yuan, Kong Xiangxin, Jiang Zaixing, et al. Sedimentary environment and organic matter enrichment of Paleogene inter-salt strata in Qianjiang sag: a case study from 10th rhythmite of the Lower Member 3 of Qianjiang Formation[J]. Acta Petrolei Sinica, 2022, 43(5): 605-616.

[126] 李志明, 孙中良, 黎茂稳, 等. 陆相基质型页岩油甜点区成熟度界限探讨: 以渤海湾盆地东营凹陷沙三下—沙四上亚段为例[J]. 石油实验地质, 2021, 43(5): 767-775.
Li Zhiming, Sun Zhongliang, Li Maowen, et al. Maturity limit of sweet spot area for continental matrix type shale oil: a case study of lower Es^3 and upper Es^4 sub-members in Dongying Sag, Bohai Bay Basin[J]. Petroleum Geology & Experiment, 2021, 43(5): 767-775.

[127] 赵语嫣. 陆相富有机质页岩储集空间与孔喉分布定量表征[D]. 北京: 中国石油大学(北京), 2019.
Zhao Yuyan. Quantitative characterization of reservoir space and pore throat distribution of continental organic-rich shale[D]. Beijing: China University of Petroleum (Beijing), 2019.

[128] 金芸芸, 李楚雄, 王勇, 等. 南襄盆地泌阳凹陷古近系核桃园组页岩含油性及烃类赋存特征[J]. 石油实验地质, 2024, 46(2): 354-365.
Jin Yunyun, Li Chuxiong, Wang Yong, et al. Oil-bearing potential and hydrocarbon occurrence characteristics of shale in Paleogene Hetaoyuan Formation in Biyang Sag, Nanxiang Basin[J]. Petroleum Geology & Experiment, 2024, 46(2): 354-365.

[129] 毛俊莉. 辽河西部凹陷页岩油气成藏机理与富集模式[D]. 北京: 中国地质大学(北京), 2020.
Mao Junli. Reservoir formation mechanism and enrichment modes of shale oil and gas in the western Liaohe Depression[D]. Beijing: China University of Geosciences (Beijing), 2020.

[130] Li S, Hu S, Xie X, et al. Assessment of shale oil potential using a new free hydrocarbon index[J]. International Journal of Coal Geology, 2016, 156: 74-85.

[131] Li M, Chen Z, Cao T, et al. Expelled oils and their impacts on Rock-Eval data interpretation, Eocene Qianjiang Formation in Jianghan Basin, China[J]. International Journal of Coal Geology, 2018, 191: 37-48.

[132] Cheng P, Xiao X, Fan Q, et al. Oil retention and its main controlling factors in lacustrine shales from the Dongying Sag, Bohai Bay Basin, Eastern China[J]. Energies, 2022, 15(12): 4270.

[133] 卢双舫, 陈国辉, 王民, 等. 辽河坳陷大民屯凹陷沙河街组四段页岩油富集资源潜力评价[J]. 石油与天然气地质, 2016, 37(1): 8-14.
Lu Shuangfang, Chen Guohui, Wang Min, et al. Potential evaluation of enriched shale oil resource of Member 4 of the Shahejie Formation in the Damintun Sag, Liaohe Depression[J]. Oil & Gas Geology, 2016, 37(1): 8-14.

[134] Song Y, Cao Q, Li S, et al. Salinized lacustrine organic-rich shale influenced by marine incursions: algal-microbial community, paleoenvironment and shale oil potential in the Paleogene Biyang Depression, East China[J]. Palaeogeography, Palaeoclimatology, Palaeoecology, 2021, 580: 110621.

[135] Wang C, Wang Q, Chen G, et al. Influence of volcanism on the development of black shales in the Chang 7 Member of Yanchang Formation in the Ordos Basin[J]. International Journal of Earth Sciences, 2021, 110(6): 1939-1960.

[136] 高可攀. 水化作用对页岩孔隙结构及声波特性的影响[J]. 天然气勘探与开发, 2025, 48(2): 39-48.
Gao Kepan. Hydration controls on pore structure and acoustic attributes in shale[J]. Natural Gas Exploration and Development, 2025, 48(2): 39-48.

[137] Kurenkov I I. The influence of volcanic ashfall on biological processes in a lake[J]. Limnology and Oceanography, 1966, 11(3): 426-429.

[138] Xiao D, Cao J, Luo B, et al. Neoproterozoic postglacial paleoenvironment and hydrocarbon potential: a review and new insights from the Doushantuo Formation Sichuan Basin, China[J]. Earth-Science Reviews, 2021, 212: 103453.

[139] Lee C A, Jiang H, Ronay E, et al. Volcanic ash as a driver of enhanced organic carbon burial in the Cretaceous[J]. Scientific Reports, 2018, 8(1): 4197.

（编辑 黄颖）